REPORT 1114

A THERMODYNAMIC STUDY OF THE TURBINE-PROPELLER ENGINE [1]

By Benjamin Pinkel and Irving M. Karp

SUMMARY

Equations and charts are presented for computing the thrust, the power output, the fuel consumption, and other performance parameters of a turbine-propeller engine for any given set of operating conditions and component efficiencies. Included are the effects of the pressure losses in the inlet duct and the combustion chamber, the variation of the physical properties of the gas as it passes through the system, and the change in mass flow of the gas by the addition of fuel.

In order to illustrate some of the turbine-propeller-system performance characteristics, the total thrust horsepower per unit mass rate of air flow and the specific fuel consumption are presented for a wide range of flight and engine-design operating conditions and a given set of design component efficiencies.

The performance of a turbine-propeller engine containing a matched set of components is presented for a range of engine operating conditions. The influence of the characteristics of the individual components on off-design-point performance is shown.

The flexibility of operation of two turbine-propeller engines is discussed; one engine has a divided turbine system in which the first turbine drives only the compressor and the second turbine independently drives the propeller, and the other engine has a connected turbine system which drives both the compressor and the propeller.

INTRODUCTION

Various thermodynamic analyses have been prepared for the purpose of studying the many aspects of the performance of turbine-propeller engines. The charts presented in reference 1, for example, permit step-by-step calculation of the turbine-propeller cycle; also presented therein are some performance characteristics of the basic turbine-propeller system and systems incorporating intercooling, reheat, and regeneration at design-point conditions. Reference 2 presents a general comparison of part-load performance characteristics of a large variety of both simple and complex turbine-propeller-engine configurations. It also discusses briefly the way in which component characteristics affect the efficiency of each engine and limit the part-load operation of each engine.

In the present report, charts (developed from an extension of the analysis given in ref. 3) are presented which permit determination of the performance parameters of the engine directly from component efficiencies and operating conditions. These charts eliminate much of the step-by-step cycle calculation and apply particularly when the engine over-all performance rather than the details of the cycle is of major interest. In order to illustrate some of the turbine-propeller-engine design-point performance characteristics, the thrust horsepower per unit mass rate of air flow and specific fuel consumption are presented for a wide range of design combustion-chamber-outlet temperatures and compressor pressure ratios. These results are presented for constant component efficiencies and a range of flight speeds and altitude conditions.

The report also presents a detailed discussion of the off-design-point performance of two turbine-propeller-engine configurations each having a given set of components. The performance of a given turbine-propeller engine is a complex function of the individual characteristics of the compressor, the turbine, and the propeller. The limitations in operating range and performance imposed by these component characteristics, the interrelation between components, some of the problems involved in matching the components, and the method for evaluating and presenting engine performance are discussed for the two engine configurations. One engine has a divided turbine system consisting of two independent turbines; the first turbine drives the compressor and the second turbine drives the propeller through reduction gears. The other engine has the two turbines connected to provide a single rotating system. The flexibility in operation provided by a variable-area exhaust nozzle is also discussed for both configurations. This analysis was made at the NACA Lewis laboratory.

SYMBOLS

The significance of the symbols appearing in the charts and in the subsequent discussion is as follows:

A_n	effective exhaust-nozzle area, sq ft (For isentropic expansion in exhaust nozzle, flow through area A_n is equal to actual mass flow through nozzle.)
a	correction factor that accounts for total-pressure drop in inlet diffuser
b	correction factor that accounts for total-pressure drop in combustion chamber
c	correction factor that accounts for difference in physical properties of hot exhaust gases and cold air, involved in computation of work from expansion process

[1] Supersedes NACA TN 2653, "A Thermodynamic Study of the Turbine-Propeller Engine," by Benjamin Pinkel and Irving M. Karp, 1952.

C_p propeller power coefficient, equal to $550\ hp_p/\rho_0 N_p^3 D_p^5$

C_v velocity coefficient of exhaust nozzle

$c_{p,a}$ specific heat of air at constant pressure at $t_0=519°$ R, 7.73 (Btu/slug)/°F

$c_{p,g}$ average specific heat at constant pressure of exhaust gases during expansion process, (Btu/slug)/°F (This term, when used with temperature change accompanying expansion, gives change in enthalpy per unit mass.)

D_p propeller diameter, ft

F total thrust, lb

F_j net thrust produced by exhaust jet, lb

F_p thrust produced by propeller, lb

f fuel-air ratio

h lower heating value of fuel, Btu/lb

hp_c compressor-shaft horsepower input

hp_p propeller-shaft horsepower input equal to excess of turbine horsepower output over compressor horsepower input

hp_t total turbine-shaft horsepower output

$hp_{t,1}$ turbine-shaft horsepower output of first turbine

J mechanical equivalent of heat, 778 ft-lb/Btu

K_c compressor slip factor, $550\ hp_c/M_a U_c^2$

M_a mass rate of air flow, slug/sec

M_g mass rate of gas flow through turbine, slug/sec

N_p propeller rotational speed, rps

P_1 total pressure at compressor inlet, lb/sq ft abs

P_2 total pressure at compressor outlet, lb/sq ft abs

P_4 total pressure at inlet to first turbine, lb/sq ft abs

P_5 total pressure at outlet of first turbine, lb/sq ft abs

P_6 total pressure at outlet of second turbine, lb/sq ft abs

p_0 ambient-static-air pressure, lb/sq ft abs

p_5 static pressure at outlet of first turbine, lb/sq ft abs

p_6 static pressure at outlet of second turbine, lb/sq ft abs

ΔP_d drop in total pressure through inlet duct, lb/sq ft

ΔP_2 drop in total pressure through combustion chamber, lb/sq ft

$(P_2/P_1)_{ref}$ factor equal to $\left[\left(\frac{1}{1+Y}\right)^2 \eta_c \eta_t \epsilon \frac{T_4}{t_0}\right]^{\frac{\gamma_a}{2(\gamma_a-1)}}$

r ratio of drop in total pressure in combustion chamber to total pressure at compressor outlet, $\Delta P_2/P_2$

T_1 compressor-inlet total temperature, °R

T_2 compressor-outlet total temperature, °R

T_4 combustion-chamber-outlet total temperature, °R

T_5 total temperature at outlet of first turbine, °R

t_0 ambient-air temperature, °R

thp total thrust horsepower produced by engine

thp_j net thrust horsepower produced by exhaust jet

thp_p thrust horsepower produced by propeller

U_c compressor tip speed, ft/sec

$U_{t,1}$ turbine blade speed (measured at turbine pitch line) of first turbine, ft/sec

$U_{t,2}$ turbine blade speed of second turbine, ft/sec

V_j jet velocity, ft/sec

$V_{j,opt}$ jet velocity giving optimum distribution of available power to propeller and exhaust-nozzle jet, ft/sec

$V_{t,1}$ theoretical turbine-nozzle jet velocity of first turbine corresponding to isentropic expansion of gas from turbine-inlet total pressure and temperature to turbine-outlet static pressure, ft/sec

$V_{t,2}$ theoretical turbine-nozzle jet velocity of second turbine, ft/sec

V_0 airplane velocity, ft/sec

V_5 axial component of gas velocity at first turbine outlet, ft/sec

V_6 axial component of gas velocity at second turbine outlet, ft/sec

W_f weight flow of fuel, lb/hr

X ratio of compressor pressure ratio, P_2/P_1 to $(P_2/P_1)_{ref}$

Y factor equal to ratio of ram temperature rise to ambient-air temperature, $V_0^2/2Jc_{p,a}t_0$

Y_j factor equal to $V_j^2/2Jc_{p,a}t_0$

Z factor equal to $550\ hp_c/M_a Jc_{p,a}t_0$

α factor equal to propeller thrust produced divided by excess of turbine horsepower output over compressor horsepower input, lb/hp

γ_a ratio of specific heats of air, 1.4

γ_g average value of ratio of specific heats of exhaust gas during expansion

δ ratio of total pressure at any point being considered to standard sea-level pressure of 2116 lb/sq ft, that is, $\delta_1=P_1/2116$, $\delta_4=P_4/2116$, and so forth

ϵ correction factor that accounts for over-all effects produced by secondary variables, $\epsilon=1-a-b+c$

η_b combustion efficiency equal to ideal fuel-air ratio required to obtain temperature rise in combustion chamber from T_2 to T_4 divided by actual fuel-air ratio

η_c compressor adiabatic efficiency equal to ideal power required in adiabatically compressing air from compressor-inlet total temperature and pressure to compressor-outlet total pressure divided by compressor-shaft power

$\eta_{c,p}$ compressor polytropic efficiency equal to logarithm of actual pressure ratio divided by logarithm of isentropic pressure ratio that corresponds to actual temperature ratio

η_p propeller efficiency equal to thrust horsepower developed by propeller divided by excess of total turbine power over compressor power. This definition includes bearing, gear, and accessory power losses as well as propeller losses.

η_t over-all turbine total efficiency of turbine system equal to entire turbine-shaft power divided by ideal power of gas jet expanding adiabatically from inlet total pressure and temperature of first turbine to outlet static pressure of second turbine less kinetic power corresponding to average axial velocity of gas at second turbine outlet

$\eta_{t,1}$ turbine total efficiency of first turbine

$\eta_{t,2}$ turbine total efficiency of second turbine

η_t' over-all turbine-shaft efficiency of turbine system equal to entire turbine-shaft power divided by ideal power of gas jet expanding adiabatically from inlet total pressure and temperature of first turbine to turbine-outlet static pressure of second turbine

$\eta_{t,1}'$ turbine-shaft efficiency of first turbine

$\eta_{t,2}'$ turbine-shaft efficiency of second turbine

θ ratio of total temperature at any point being considered to standard sea-level temperature of 519° R, that is, $\theta_1=T_1/519$, $\theta_4=T_4/519$, and so forth

ρ_0 density of ambient air, slug/cu ft

ANALYSIS

A schematic diagram of the turbine-propeller engine considered is shown in figure 1. Air enters the inlet duct and passes to the compressor inlet. Part of the dynamic pressure of the free-air stream is converted into static pressure at the compressor inlet by the diffusing action of the inlet duct. The air is further compressed in passing through the compressor and enters the combustion chamber where fuel is injected and burned. The products of combustion then pass through the turbine nozzles and blades, where an appreciable drop in pressure occurs, and finally are discharged rearwardly through the exhaust nozzle to provide jet thrust. The turbine shown in figure 1 may consist of a single turbine driving both the compressor and the propeller or a combination of two turbines, one driving the compressor and another driving the propeller. When engine performance is evaluated by charts, the combination of the two turbines is considered as a single turbine having the combined power output and over-all turbine efficiency of the two.

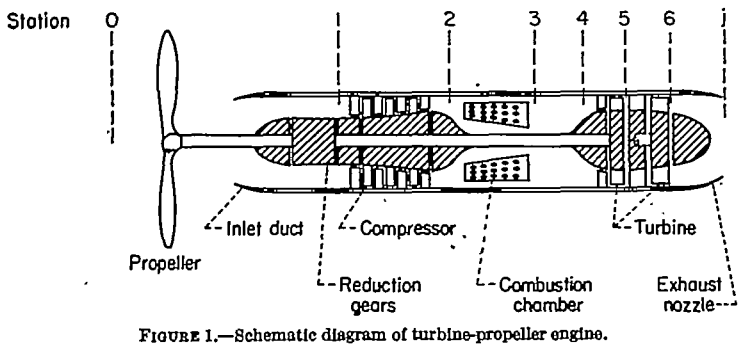

FIGURE 1.—Schematic diagram of turbine-propeller engine.

The variables affecting the performance are divided into a primary group and a secondary group.

The primary group of variables is:

- Exhaust-nozzle velocity coefficient, which includes losses in tail pipe, C_v
- Compressor total-pressure ratio, P_2/P_1
- Combustion-chamber-outlet total temperature, T_4
- Ambient-air temperature, t_0
- Jet velocity, V_j
- Airplane velocity, V_0
- Ratio of propeller thrust produced to propeller-shaft horsepower input, α
- Burner efficiency, η_b
- Compressor adiabatic efficiency, η_c
- Propeller efficiency, which includes losses in reduction gearing, η_p
- Turbine total efficiency, η_t

The secondary group is:

- Ratio of total-pressure drop through inlet duct to compressor-inlet total pressure, $\Delta P_d/P_1$
- Ratio of total-pressure drop through combustion chamber to compressor-outlet total pressure, $\Delta P_2/P_2$
- Effect of difference between physical properties of cold air and hot exhaust gases during expansion processes. (Effect of change in specific heat of gas during other processes is included in charts.)

Charts are presented from which the propeller-thrust horsepower, the propeller thrust, and the fuel-air ratio can be evaluated for various combinations of design-point operating conditions. The equations from which the charts are prepared are derived in appendix A and are listed in appendix B. Some of the following equations used in combination with the charts give the performance of the turbine-propeller system.

The total thrust of the engine is the sum of the propeller thrust and the jet thrust.

The jet thrust, when the effect of the added fuel is neglected, is given by

$$F_j=M_a(V_j-V_0) \tag{1a}$$

When the effect of added fuel is included, the jet thrust is given by

$$F_j=M_a(V_j-V_0)+fM_aV_j \tag{1b}$$

The thrust horsepower of the jet is expressed as

$$thp_j=\frac{F_jV_0}{550} \tag{2}$$

The thrust horsepower produced by the propeller (which includes the effect of added fuel) is given by

$$thp_p=\frac{M_a\eta_pJc_{p,a}t_0}{550}\left[\eta_t(1+f)\frac{T_4}{t_0}\epsilon\frac{Y+\eta_cZ}{1+Y+\eta_cZ}-\frac{V_j^2\eta_t(1+f)}{2C_v^2Jc_{p,a}t_0}-Z\right] \tag{3}$$

and can be evaluated from the charts.

The total thrust horsepower of the engine is the sum of the jet-thrust horsepower and propeller-thrust horsepower.

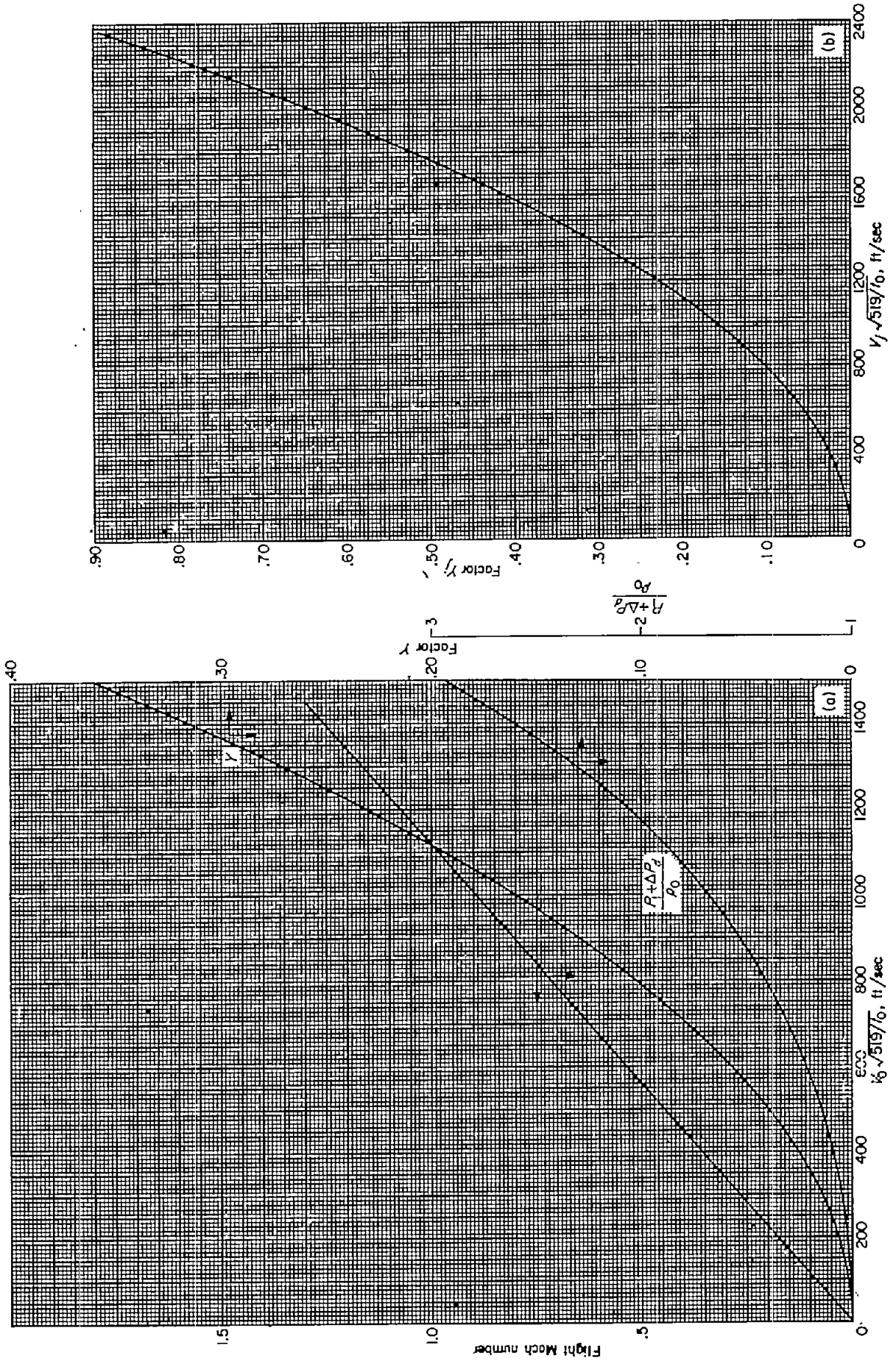

(a) Flight Mach number, factor Y, and $\frac{P_1+\Delta P_d}{P_0}$.

(b) Factor Y_f.

FIGURE 2.—Charts for determining flight Mach number, compressor-inlet total pressure, and factors Y and Y_f.

For the engine operating at a given set of conditions, an optimum division of power between the exhaust jet and the propeller exists for which the total thrust horsepower and efficiency of the system are maximum. The jet velocity for this optimum condition is given very closely by

$$V_{j,opt}=\frac{C_v^2}{\eta_t\eta_p}V_0 \tag{4a}$$

This expression is derived in appendix A. The jet velocity can vary appreciably from this optimum value with only a small effect on the total thrust horsepower and engine efficiency.

At zero flight speed ($V_0=0$ and $\eta_p=0$) the expression for $V_{j,opt}$ is indeterminate. When the factor α is introduced where α is the pounds of thrust produced by the propeller per propeller-shaft horsepower input, the expression for $V_{j,opt}$ becomes

$$V_{j,opt}=\frac{550C_v^2}{\eta_t\alpha} \tag{4b}$$

The thrust developed by the propeller at any plane speed V_0 ($V_0\neq 0$) is obtained from the propeller-thrust horsepower by the equation

$$F_p=thp_p\frac{550}{V_0} \tag{5}$$

For the case of $V_0=0$, the factor F_p/α is determined from the charts.

The compressor-shaft horsepower is given by

$$hp_c=M_aJc_{p,a}t_0Z/550=5675M_aZt_0/519 \tag{6}$$

The compressor-inlet total temperature is

$$T_1=t_0(1+Y) \tag{7}$$

The turbine-shaft horsepower is

$$hp_t=\frac{thp_p}{\eta_p}+hp_c \tag{8a}$$

At zero flight speed ($thp_p=0$ and $\eta_p=0$), the turbine power is

$$hp_t=\frac{F_p}{\alpha}+hp_c \tag{8b}$$

The fuel consumption per unit mass rate of air flow is determined from the fuel-air ratio by the relation

$$W_f/M_a=115{,}900f \tag{9}$$

DISCUSSION OF CHARTS

By means of equations (1) to (9) and the curves of figures 2 to 7, the performance of the turbine-propeller engine can be readily evaluated. The curves are presented in a form that shows the effects of the variables on performance. In figures 2 to 4 are shown curves for evaluating some of the primary parameters that are used in the principal performance chart (fig. 5) from which the thrust horsepower of the propeller is determined. The fuel-air ratio is evaluated with the use of figures 6 and 7.

Curves for obtaining the flight Mach number, the compressor-inlet total pressure, and the factor Y for various values of the factor $V_0\sqrt{519/t_0}$ are shown in figure 2 (a). Values of Y_f plotted against the factor $V_f\sqrt{519/t_0}$ are shown in figure 2 (b).

The value of ϵ, which accounts for the effect of the secondary group of variables, is obtained from figure 3. The quantity ϵ is given by the relation

$$\epsilon=1-a-b+c$$

Correction a, which gives the effect of total-pressure drop through the inlet duct ΔP_d, is shown in figure 3 (a). Cor-

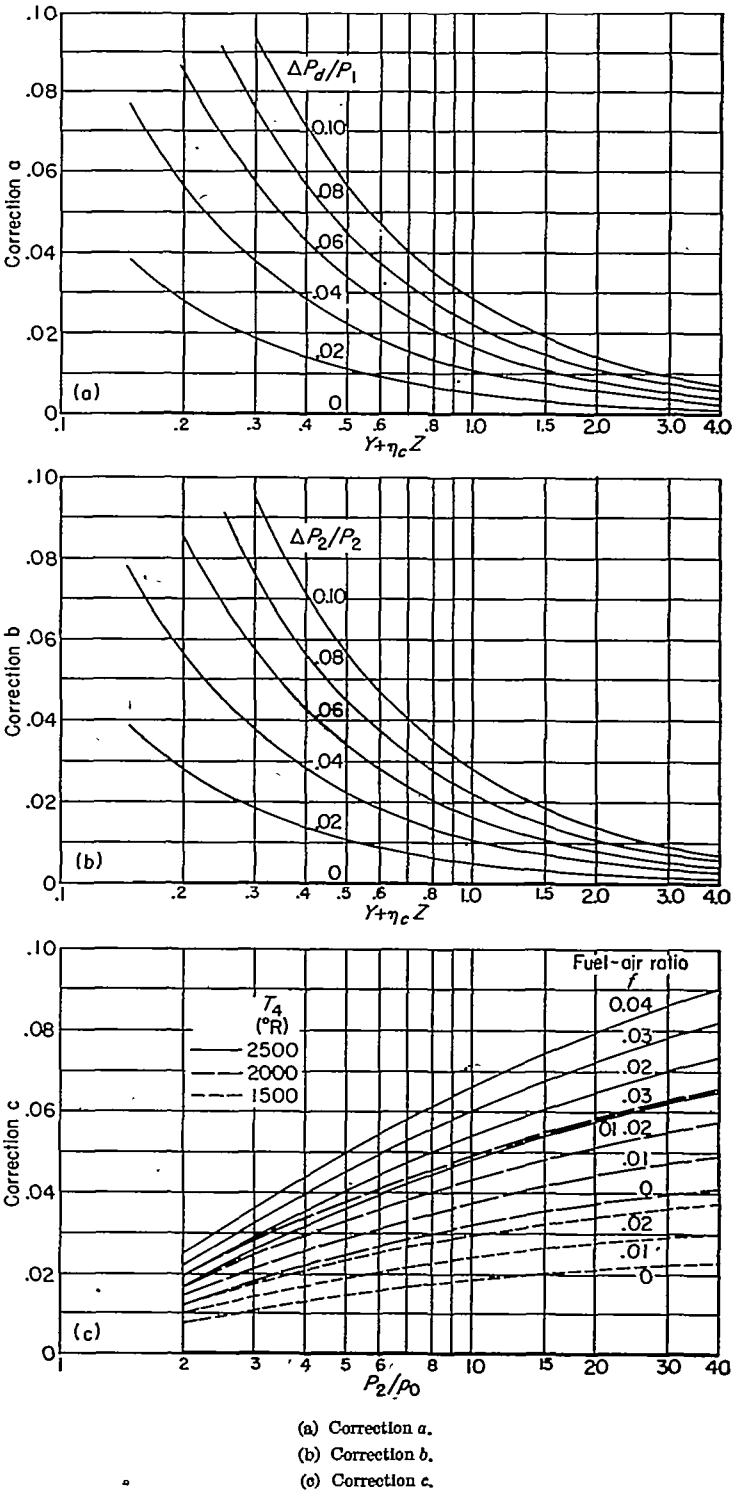

(a) Correction a.
(b) Correction b.
(c) Correction c.

FIGURE 3.—Chart for determining factor ϵ. ($\epsilon=1-a-b+c$)

rection b, which measures the effect of total-pressure drop through the combustion chamber ΔP_2, is introduced in figure 3 (b). Correction c, which corrects for the difference between the physical properties of the hot exhaust gases and the cold air involved in the computation of the expansion processes through the turbine and exhaust nozzle, is given in figure 3 (c). In general, the value of ϵ is close to unity and can be taken as equal to unity when a rapid approximation is desired.

The compressor total-pressure ratio is plotted against the quantity $\eta_c Z/(1+Y)$ in figure 4. The compressor-shaft horsepower is computed from equation (6) and the value of Z. The effect of the variation in specific heat of air during compression is neglected in this plot; the maximum error in Z introduced is about 1 percent for the range of compressor pressure ratios shown in figure 4 and for compressor-inlet temperatures up to 550° R.

The value of $(P_2/P_1)_{ref}$ plotted against the factor $\eta_c\eta_t\epsilon\frac{T_4}{t_0}\left(\frac{1}{1+Y}\right)^2$ is also shown in figure 4. The quantity $(P_2/P_1)_{ref}$ is useful in that it is the compressor pressure ratio for maximum power per unit mass rate of air flow for any given values of $\eta_c\eta_t\epsilon T_4/t_0$ and Y, provided that the change in component efficiencies and ϵ with change in pressure ratio is negligible. When the change in ϵ with P_2/P_1 is appreciable, $(P_2/P_1)_{ref}$ differs somewhat from the compressor pressure ratio giving maximum power per unit mass rate of air flow. Even in this case, the power per unit mass rate of air flow corresponding to $(P_2/P_1)_{ref}$ is generally within 1 percent of the true maximum. The actual compressor pressure ratio P_2/P_1 divided by the quantity $(P_2/P_1)_{ref}$ defines the value of X used in figure 5.

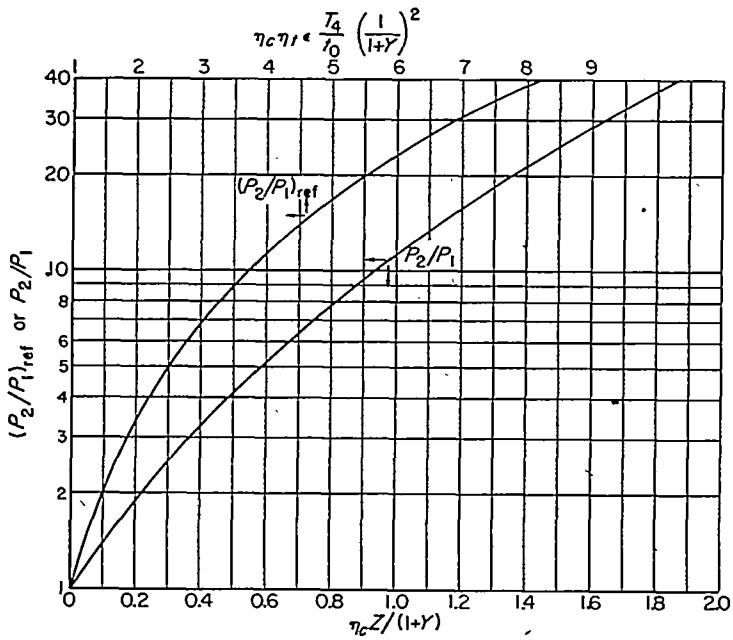

FIGURE 4.—Chart for determining $(P_2/P_1)_{ref}$ for various values of $\eta_c\eta_t\epsilon\frac{T_4}{t_0}\left(\frac{1}{1+Y}\right)^2$ and for determining $\frac{\eta_c Z}{1+Y}$ for various values of P_2/P_1. (A 17- by 19-in. print of this chart is available from NACA upon request.)

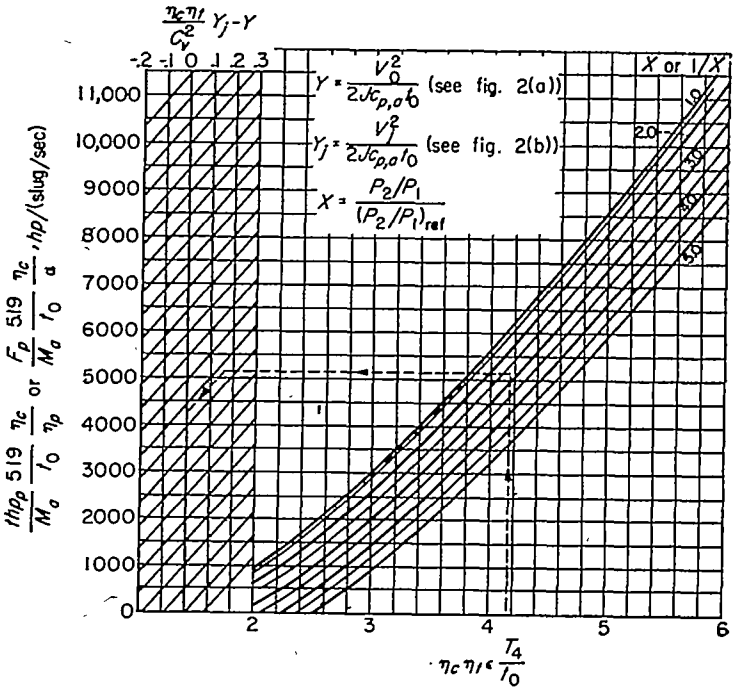

FIGURE 5.—Chart for determining thrust-horsepower or shaft-horsepower factors. (A 17- by 21-in. print of this chart (in two sections) is available from NACA upon request.)

The curves in figure 5 are used to determine the propeller-horsepower factors $\frac{thp_p}{M_a}\frac{519}{t_0}\frac{\eta_c}{\eta_p}$ or $\frac{F_p}{M_a}\frac{519}{t_0}\frac{\eta_c}{\alpha}$ for various values of the parameters $\eta_c\eta_t\epsilon T_4/t_0$, $(\eta_c\eta_t/C_v^2)Y_j-Y$, and X or $1/X$. When X is less than unity, the value of $1/X$ is used; the reason is apparent from an examination of equation (A34) (see appendix B) for figure 5. Corresponding to the values of $\eta_c\eta_t\epsilon T_4/t_0$ and X or $1/X$, a point on the right-hand set of curves is determined; then progressing horizontally across the chart to the desired value of $(\eta_c\eta_t/C_v^2)Y_j-Y$, a second point is located. Moving from this second point parallel to the left-hand set of direction lines until the $(\eta_c\eta_t/C_v^2)Y_j-Y=0$ line is intercepted, the value of the propeller-thrust-horsepower factor or propeller-shaft-horsepower factor is then read at the intercept.

The compressor-outlet total temperature T_2 plotted against the factor $t_0(1+Y+Z)$ is shown in figure 6. This curve includes the variation in specific heat of air during compression and was computed from reference 4. The variation in specific heat is accounted for in this case; whereas it is neglected in figure 4, because the error introduced in the evaluation of the temperature rise during compression by the assumption of a constant value of specific heat is greater than the error introduced by the same assumption in the evaluation of the compressor power.

The fuel-air-ratio factor $\eta_b f$ is plotted in figure 7 against T_4-T_2 (total-temperature rise in combustion chamber) for various values of T_4. These curves are based on information given in reference 5 and are for a fuel having a lower heating value h of 18,900 Btu per pound and a hydrogen-carbon ratio of 0.185. For fuels having other values of h, the value of f given in figure 7 is corrected accurately by multiplying it by

the factor 18,900/h. The effect of hydrogen-carbon ratio of fuel on f is generally small; and, for a range of hydrogen-carbon ratios from 0.16 to 0.21, the error due to the deviation from the value of 0.185 is less than 0.5 percent. The fuel consumption per unit mass rate of air flow is obtained from the value of f and equation (9).

In the preceding discussion of the charts, the effect of the mass of injected fuel was not mentioned. It is shown in appendix A that the effect of the added fuel can be taken into account by substituting the product of turbine total efficiency η_t and $(1+f)$ for the value of η_t in the charts. This adjustment occurs in figure 4 in the factor $\eta_c\eta_t\epsilon\frac{T_4}{t_0}\left(\frac{1}{1+Y}\right)^2$ (which is used in determining $(P_2/P_1)_{ref}$) and in the factors $\eta_c\eta_t\epsilon T_4/t_0$ and $(\eta_c\eta_t/C_v^2)Y_j-Y$ of figure 5. The value of the jet-thrust horsepower is evaluated from the jet velocity by means of equations (1b) and (2). Equations (4a) and (4b), which are used to determine the optimum jet velocity, do not require this adjustment in the value of η_t.

EXAMPLES OF USE OF CHARTS

As an example of the use of figures 2, 4, and 5 and equations (1) and (2) for a rapid approximate computation of the thrust horsepower per unit mass rate of air flow thp/M_a, a case is considered in which the following conditions are given:

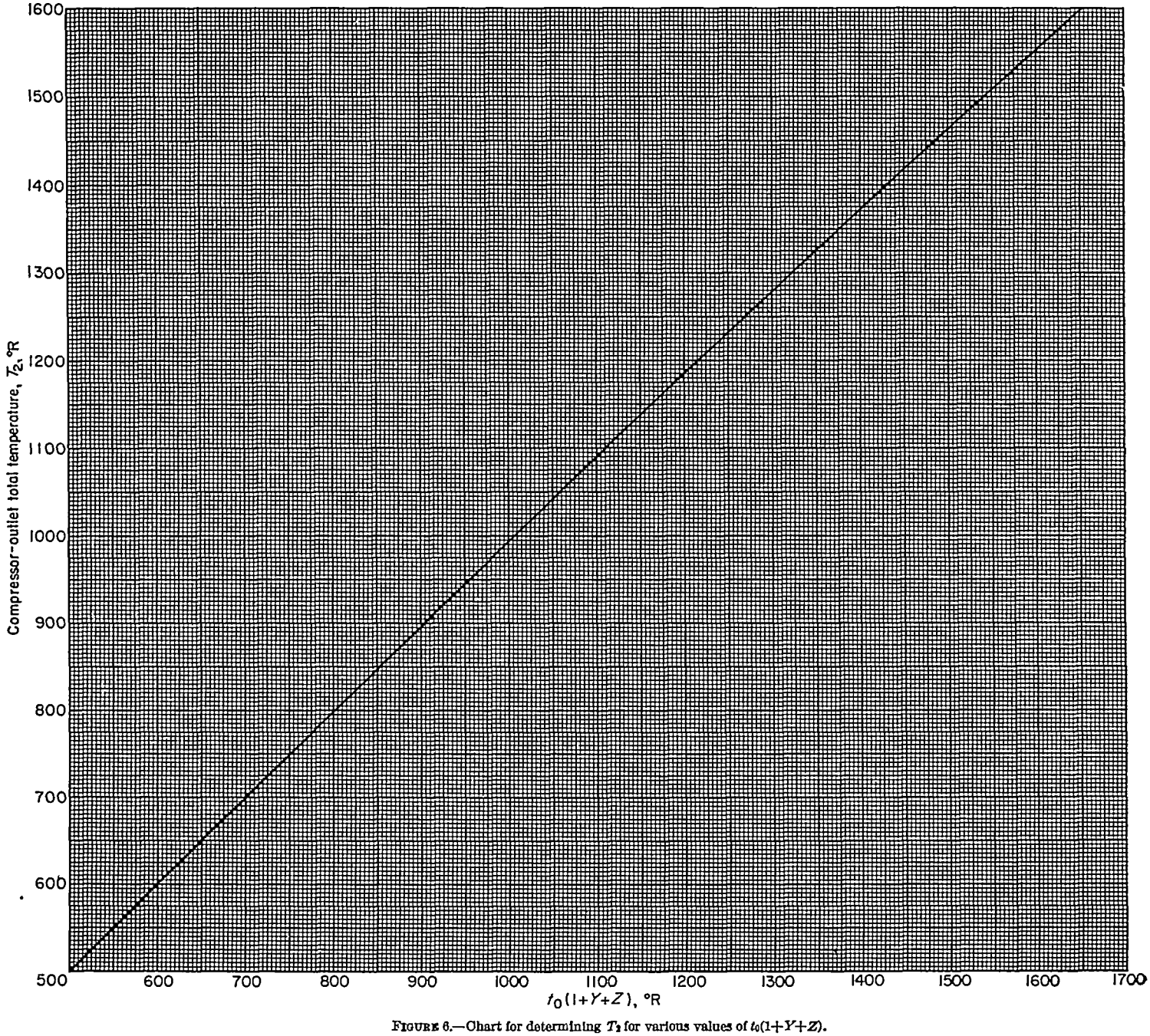

FIGURE 6.—Chart for determining T_2 for various values of $t_0(1+Y+Z)$.

Compressor adiabatic efficiency, η_c	0. 80
Turbine total efficiency, η_t	0. 90
Propeller efficiency, η_p	0. 85
Exhaust-nozzle velocity coefficient, C_v	0. 96
Airplane velocity, V_0, ft/sec	733
Jet velocity, V_j, ft/sec	1000
Compressor pressure ratio, P_2/P_1	6
Ambient-air temperature, t_0, °R	519
Combustion-chamber-outlet temperature, T_4, °R	1960

From the assumption that ϵ is equal to 1, thp/M_a is then evaluated with these given quantities as follows:

$V_0\sqrt{519/t_0}$, ft/sec	733
Y (from fig. 2 (a))	0. 086
$V_j\sqrt{519/t_0}$, ft/sec	1000
Y_j (from fig. 2 (b))	0. 160
$\eta_c\eta_t\epsilon T_4/t_0$	2. 719
$\eta_c\eta_t\epsilon\frac{T_4}{t_0}\left(\frac{1}{1+Y}\right)^2$	2. 305
$(P_2/P_1)_{ref}$ (from fig. 4)	4. 31
$X=(P_2/P_1)/(P_2/P_1)_{ref}$	1. 39
$(\eta_c\eta_t/C_v^2)Y_j-Y$	0. 039
$\frac{thp_p}{M_a}\frac{\eta_c}{\eta_p}\frac{519}{t_0}$, hp/(slug/sec) (from fig. 5)	2085
thp_p/M_a, hp/(slug/sec)	2215
thp_j/M_a, hp/(slug/sec) (from eqs. (1) and (2))	355
thp/M_a, hp/(slug/sec)	2570

The use of figures 2 to 7 and equations (1) to (9), which permit evaluation of such performance values as compressor-shaft power, fuel consumption, thrust horsepower, and specific fuel consumption with a high degree of accuracy, is illustrated in detail in the following example. The effects of the secondary parameters are now accurately evaluated and the method of accounting for added fuel mass is also shown. The example is based on the engine having the following design conditions:

(1) Compressor adiabatic efficiency, η_c	0. 80
(2) Turbine total efficiency, η_t	0. 90
(3) Combustion efficiency, η_b	0. 97
(4) Propeller efficiency, η_p	0. 85
(5) Exhaust-nozzle velocity coefficient, C_v	0. 96
(6) Airplane velocity, V_0, ft/sec	733
(7) Jet velocity, V_j, ft/sec	1000
(8) Compressor total-pressure ratio, P_2/P_1	6
(9) Ambient-air temperature, t_0, °R	519
(10) Combustion-chamber-outlet total temperature, T_4, °R	1960
(11) Ambient-air pressure, p_0, lb/sq in.	14. 7
(12) Total-pressure drop through inlet duct, ΔP_d, lb/sq in.	0. 25
(13) Total-pressure drop through combustion chamber, ΔP_2, lb/sq in.	1. 5
(14) Lower heating value of fuel, h, Btu/lb	18,500

DETERMINATION OF Y AND FLIGHT MACH NUMBER

From items (6) and (9):

(15) $V_0\sqrt{519/t_0}$, ft/sec	733

From item (15) and figure 2 (a):

(16) Y	0. 086
(17) Flight Mach number	0. 66

DETERMINATION OF Z AND hp_d/M_a

Item (8) read on figure 4 determines

(18) $\eta_cZ/(1+Y)$	0. 669

From items (18), (16), and (1):

(19) Z	0. 908

Using items (19) and (9) in equation (6) gives

(20) hp_d/M_a, hp/(slug/sec)	5153

DETERMINATION OF f AND W_f/M_a

From items (9), (16), and (19):

(21) $t_0(1+Y+Z)$, °R	1035

From item (21) read on figure 6:

(22) T_2, °R	1025

From items (22) and (10):

(23) T_4-T_2, °R	935

From items (23) and (10) and figure 7:

(24) η_bf	0. 01372

Items (24) and (3) give

(25) f	0. 01414

Because the lower heating value of the fuel is equal to 18,500 Btu per pound (item (14)), item (25) must be multiplied by the factor 18,900/18,500, and the adjusted value is

(26) f	0. 01445

Using item (26) in equation (9) gives

(27) W_f/M_a, (lb/hr)/(slug/sec)	1675

DETERMINATION OF FACTOR ϵ

From items (11), (12), and (13):

(28) $\Delta P_d/p_0$	0. 017
(29) $\Delta P_2/p_0$	0. 10

From figure 2 and item (15):

(30) $(P_1+\Delta P_d)/p_0$	1. 335

and using item (28) with item (30) gives

(31) P_1/p_0	1. 318

Using items (31) and (8) yields

(32) P_2/p_0	7. 91

From items (28) and (31):

(33) $\Delta P_d/P_1$	0. 013

whereas from items (29) and (32):

(34) $\Delta P_2/P_2$	0. 013

From items (16) and (18):

(35) $Y+\eta_cZ$	0. 812

Items (33) and (35) in figure 3 (a) give

(36) a	0. 005

while items (34) and (35) in figure 3 (b) give

(37) b	0. 005

When items (10), (26), and (32) are used in figure 3 (c),

(38) c	0. 035

From items (36), (37), and (38):

(39) $\epsilon=1-0.005-0.005+0.035$	1. 025

DETERMINATION OF $(P_2/P_1)_{ref}$ AND X

Using items (1), (2), (39), (10), (9), and (16) gives

(40) $\eta_c\eta_t\epsilon\frac{T_4}{t_0}\left(\frac{1}{1+Y}\right)^2$	2. 363

From item (40) read on figure 4:

(41) $(P_2/P_1)_{ref}$	4. 50

From items (8) and (41) and the definition of the parameter X,

(42) X	1. 333

DETERMINATION OF thp/M_a, SPECIFIC FUEL CONSUMPTION, AND OTHER PERFORMANCE PARAMETERS

Using items (1), (2), (39), (10), and (9) gives

(43) $\eta_c\eta_t\epsilon T_4/t_0$	2. 787

From items (7) and (9):

(44) $V_j\sqrt{519/t_0}$, ft/sec	1000

and from item (44) read on figure 2 (b):

(45) Y_j	0. 160

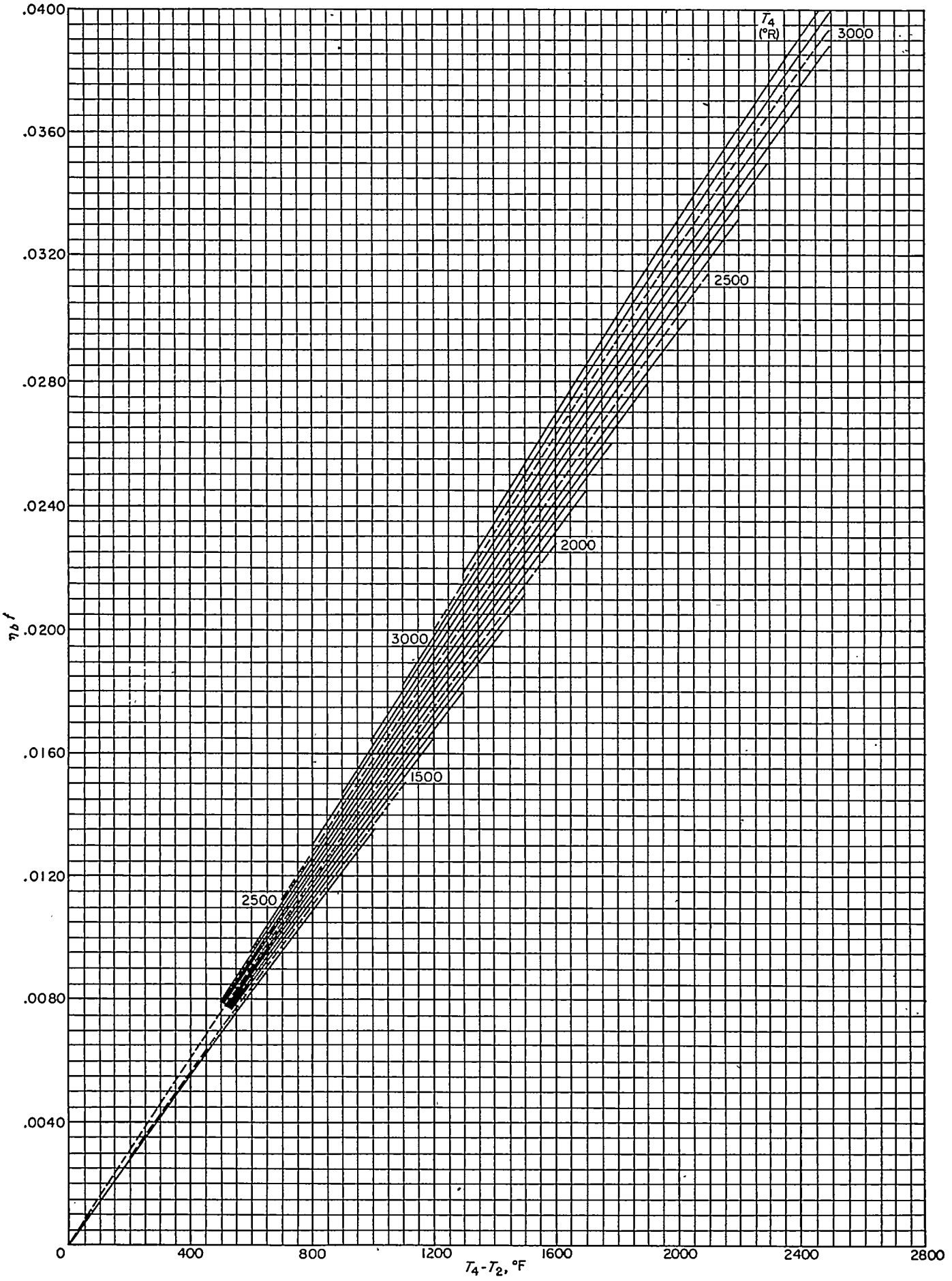

FIGURE 7.—Chart for determining f for various values of $T_4 - T_2$ and T_4; h, 18,900 Btu per pound; hydrogen-carbon ratio, 0.185. (A 15- by 21-in. print of this chart is available from NACA upon request.)

From items (1), (2), (5), (45), and (16):

(46) $\eta_c\eta_t Y_j/C_3^2 - Y$ ---------- 0.039

From items (46), (43), and (42), read on figure 5:

(47) $\frac{thp_p}{M_a}\frac{\eta_c}{\eta_p}\frac{519}{t_0}$, hp/(slug/sec) ---------- 2257

The thrust horsepower per unit mass rate of air flow developed by the propeller is obtained by using items (47), (1), (4), and (9):

(48) thp_p/M_a, hp/(slug/sec) ---------- 2399

Items (48) and (6) are substituted in equation (5); the thrust per unit mass rate of air flow developed by the propeller is

(49) F_p/M_a, lb/(slug/sec) ---------- 1799

Using items (6) and (7) in equation (1a) gives

(50) F_j/M_a, lb/(slug/sec) ---------- 267

and then items (50) and (6) in equation (2) give

(51) thp_j/M_a, hp/(slug/sec) ---------- 356

Now, from items (48) and (51):

(52) thp/M_a, hp/(slug/sec) ---------- 2755

and from items (49) and (50):

(53) F/M_a, lb/(slug/sec) ---------- 2066

The specific fuel consumption is evaluated from items (27) and (52):

(54) W_f/thp, lb/hp-hr ---------- 0.608

EFFECT OF MASS OF ADDED FUEL ON F/M_a AND thp/M_a

When more accurate results are desired, the effect of the mass of fuel introduced is accounted for in the calculations. The effect of the added fuel is handled by substituting the product of the turbine total efficiency η_t and $(1+f)$ for the value of η_t, which will now be done for the case just considered.

From item (26) the adjusted value of item (40) becomes

(55) $\eta_c\eta_t\epsilon\frac{T_4}{t_0}\left(\frac{1}{1+Y}\right)^2$ ---------- 2.396

From figure 4 is obtained the corresponding

(56) $(P_2/P_1)_{ref}$ ---------- 4.61

From items (56) and (8):

(57) X ---------- 1.30

By use of the modified value of η_t, item (43) becomes

(58) $\eta_c\eta_t\epsilon T_4/t_0$ ---------- 2.827

and item (46) becomes

(59) $\eta_c\eta_t Y_j/C_3^2 - Y$ ---------- 0.0410

Using items (57), (58), and (59) in figure 5 gives

(60) $\frac{thp_p}{M_a}\frac{\eta_c}{\eta_p}\frac{519}{t_0}$, hp/(slug/sec) ---------- 2351

or

(61) thp_p/M_a, hp/(slug/sec) ---------- 2497

Evaluating the propeller thrust from items (61) and (6) and from equation (5) gives

(62) F_p/M_a, lb/(slug/sec) ---------- 1874

In evaluating the jet thrust from items (6) and (7), equation (1b) is now used and gives

(63) F_j/M_a, lb/(slug/sec) ---------- 281

From items (63) and (6) and from equation (2):

(64) thp_j/M_a, hp/(slug/sec) ---------- 375

The total thrust horsepower per unit mass rate of air flow from items (61) and (64) is

(65) thp/M_a, hp/(slug/sec) ---------- 2872

From items (62) and (63):

(66) F/M_a, lb/(slug/sec) ---------- 2155

and from items (65) and (27):

(67) W_f/thp, lb/thp-hr ---------- 0.583

ACCURACY OF METHOD

The final equations for thrust horsepower (eqs. (A24) and (A34)), from which figure 5 is plotted and which are derived with the aid of several simplifying assumptions, give values of thrust horsepower which check very closely with values obtained from very accurate step-by-step evaluation of conditions throughout the cycle. Over a wide range of operating and flight conditions, the maximum error in the value of thrust horsepower obtained from the charts is less than 0.5 percent.

The results of the examples used to illustrate the use of the charts give an indication of the effect of ϵ on the thrust horsepower. For the conditions of the example, choosing an approximate value of $\epsilon=1.0$ results in a value of thrust horsepower about 7 percent different from the value of thrust horsepower evaluated from the more accurate value of $\epsilon=1.025$. In general, the percentage error in thrust horsepower will range from two to four times the percentage error in ϵ. In cases where the combination of conditions is such as to result in low values of thrust horsepower, an error in ϵ has a much greater effect on thrust horsepower.

Also, for the set of conditions chosen, the thrust power is about 4 percent greater and the specific fuel consumption about 4 percent lower when the added mass of fuel is taken into account. In general, if good accuracy of results is desired from the charts, it is necessary to include the effect of added fuel.

TURBINE-PROPELLER-ENGINE PERFORMANCE

In order to illustrate the performance and some of the characteristics of the turbine-propeller engine, several cases are presented. First, the performance of the turbine-propeller system over a range of flight and engine-design-point operating conditions and fixed design-point component efficiencies is discussed. Each set of design-point operating conditions and component efficiencies represents a different engine. Second, the off-design-point performance of two specific turbine-propeller engines (with given sets of matched components) is discussed. For this case a method is presented for matching components; also the interrelation between component characteristics and over-all engine performance is shown.

DESIGN-POINT ENGINES

For the purpose of illustrating the manner in which the thrust horsepower per unit mass rate of air flow and specific fuel consumption are influenced by compressor pressure ratio, combustion-chamber-outlet temperature, flight speed, and ambient-air temperature, the following fixed parameters are assumed:

Compressor adiabatic efficiency, η_c	0.85
Turbine total efficiency, η_t	0.90
Combustion efficiency, η_b	0.96
Propeller efficiency, η_p	0.85
Exhaust-nozzle velocity coefficient, C_v	0.97
Lower heating value of fuel, h, Btu/lb	18,900
Correction factor, ϵ	1.00

The jet velocities in all cases considered were the optimum jet velocities evaluated from equations (4a) and (4b).

The effect of the mass of fuel added is included in these performance calculations.

The values of component efficiencies and ϵ at the design point will tend to vary with change in design-point operating conditions. In the present computations, the component efficiencies and ϵ were assumed constant at the values listed. The method illustrated in the examples for using the charts was followed in evaluating the performance.

The performance of the system is presented in figure 8; the thrust horsepower per unit mass rate of air flow (or equivalent propeller shaft horsepower per unit mass rate of

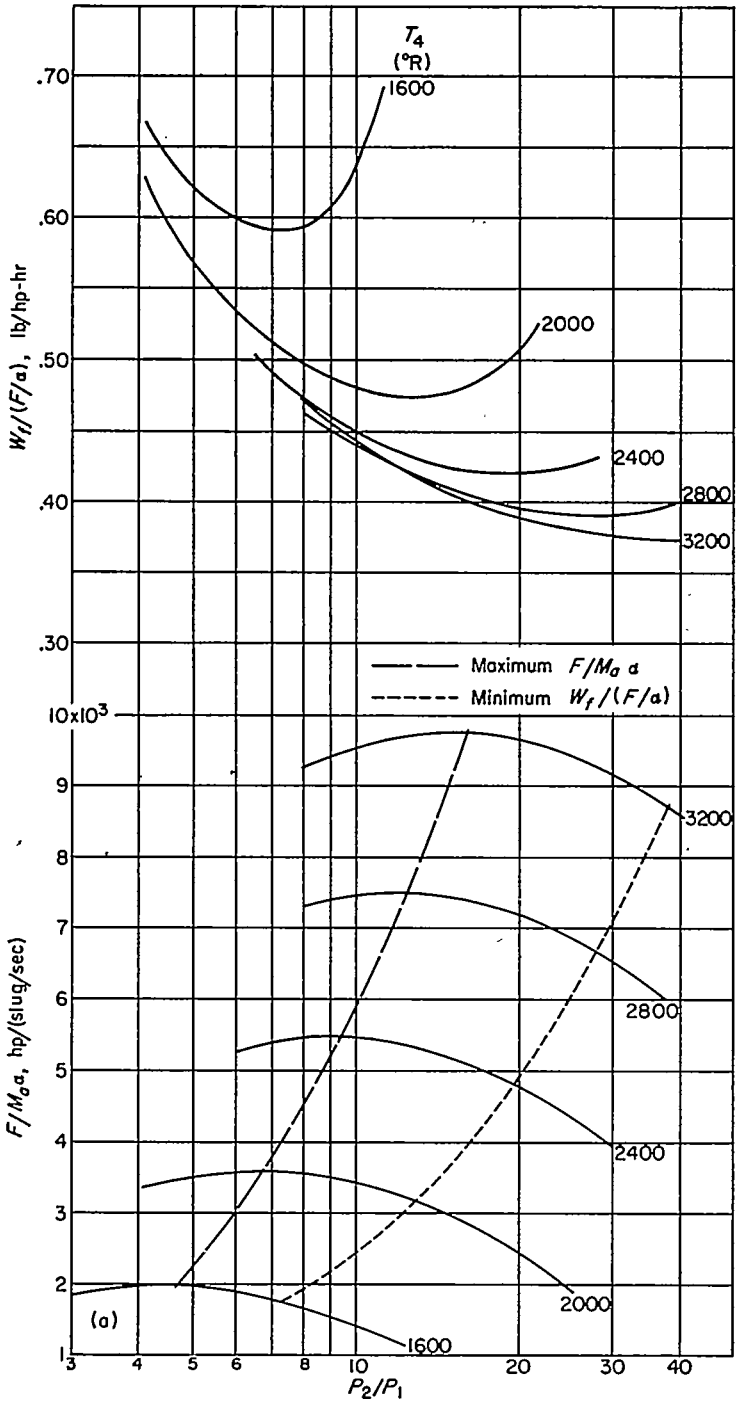

(a) V_0, 0; t_0, 519° R; V_j, 144 feet per second; α, 4 pounds thrust per horsepower (to convert jet thrust to equivalent shaft horsepower).

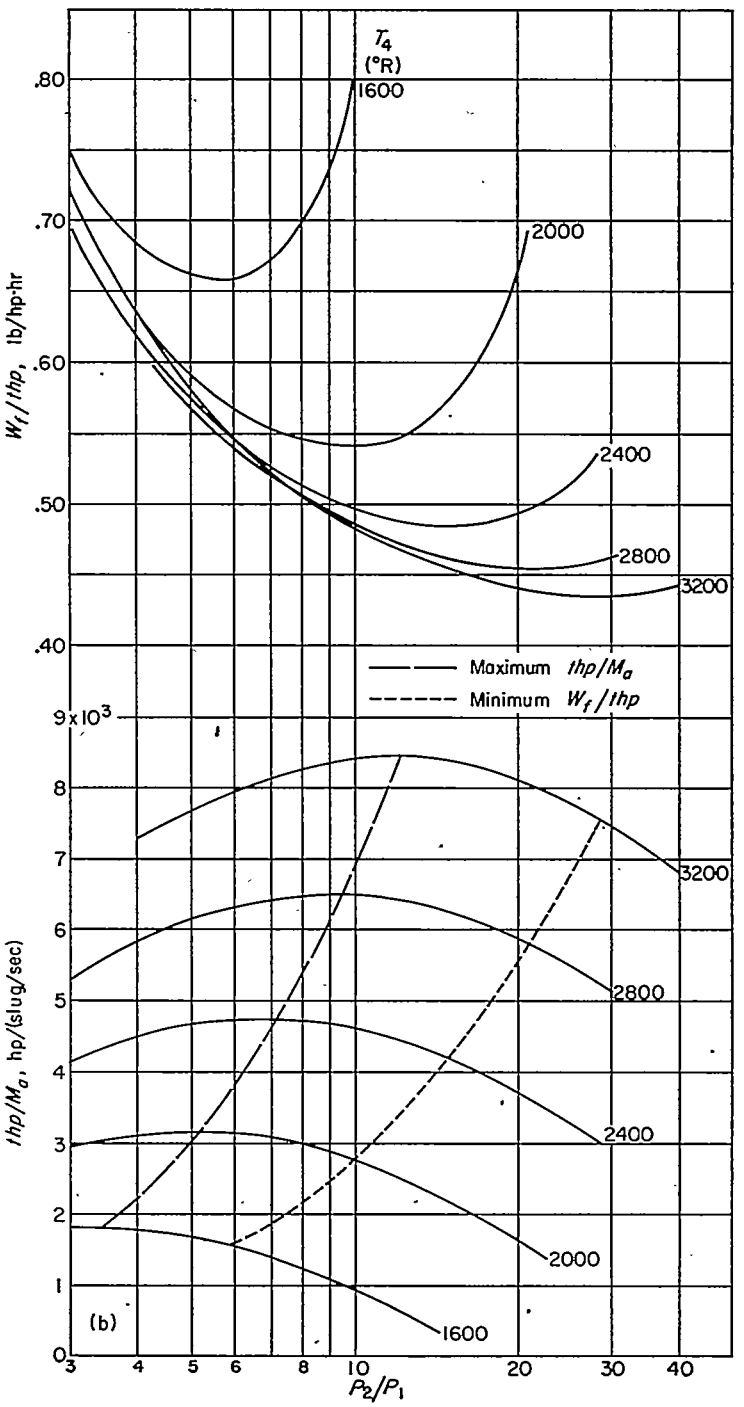

(b) V_0, 733 feet per second; t_0, 519° R; V_j, 902 feet per second; η_p, 0.85.

FIGURE 8.—Performance of turbine-propeller engines for range of design-point flight and engine operating conditions; η_c, 0.85; η_t, 0.90; η_b, 0.96; C_v, 0.97; h, 18,900 Btu per pound; ϵ, 1.00.

air flow for the static case, $V_0=0$) and the specific fuel consumption are plotted against compressor pressure ratio for various values of combustion-chamber-outlet temperature at several combinations of airplane velocity and ambient-air temperature. The range of T_4 investigated was from 1600° to 3200° R, and the compressor pressure ratios ranged up to 40. Lines for compressor pressure ratios giving maximum thrust horsepower per unit mass rate of air flow ($X=1$) and for minimum specific fuel consumption at any temperature T_4 are included in the figure.

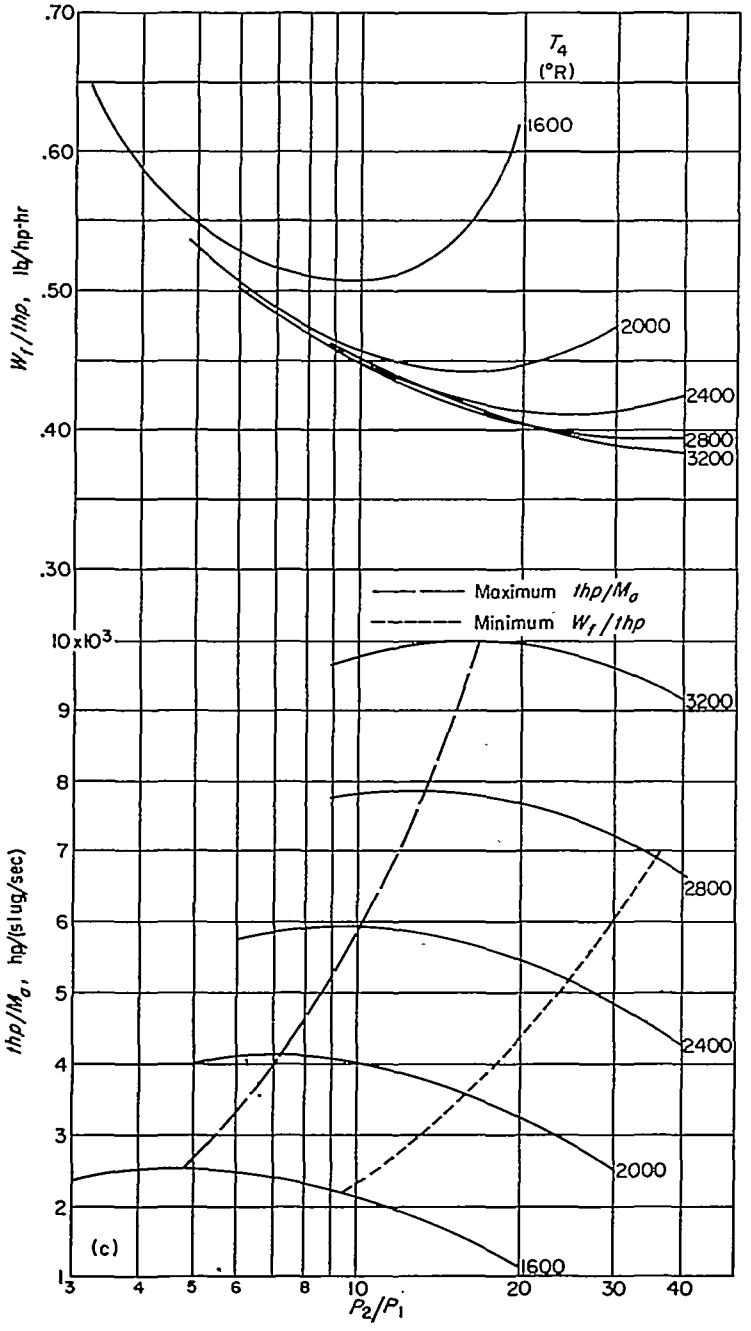

(c) V_0, 733 feet per second; t_0, 412° R; V_j, 902 feet per second; η_p, 0.85.

FIGURE 8.—Concluded. Performance of turbine-propeller engines for range of design-point flight and engine operating conditions; η_c, 0.85; η_t, 0.90; η_b, 0.96; C_t, 0.97; h, 18,900 Btu per pound; ϵ, 1.00.

Performance curves at $V_0=0$ and $t_0=519°$ R are shown in figure 8 (a). For this case where the thrust horsepower is zero, the equivalent total shaft power per unit mass rate of air flow $F/M_a\alpha$ and specific fuel consumption based on equivalent shaft power are plotted against compressor pressure ratio. The factor α was assumed equal to 4 pounds per horsepower in order to convert the jet thrust into equivalent shaft power. The optimum jet velocity calculated from equation (4b) for this case is 144 feet per second.

In figures 8 (b) and 8 (c) are presented curves of thrust horsepower per unit mass rate of air flow and of specific fuel consumption plotted against compressor pressure ratio. Figure 8 (b) is for the case of $V_0=733$ feet per second and $t_0=519°$ R; and figure 8 (c), for $V_0=733$ feet per second and $t_0=412°$ R. The optimum jet velocity for both these cases, computed from equation (4a), is 902 feet per second.

The curves of figure 8 show that with no limitation on compressor pressure ratio, higher thp/M_a (or equivalent total shaft power per unit mass rate of air flow when the system is at rest) and lower specific fuel consumption can be obtained by increasing the T_4. At any given T_4 there is an optimum P_2/P_1 for maximum thp/M_a and an optimum P_2/P_1 for minimum W_f/thp. The compressor pressure ratio for minimum specific fuel consumption is greater than that required for maximum thp/M_a.

The effects of flight speed and ambient-air temperature on the performance of the turbine-propeller system at a given combustion-chamber-outlet temperature of 1960° R are shown in figure 9. In figure 9 (a), the thp/M_a and W_f/thp are plotted against ambient-air temperatures at V_0 of 367 and 733 feet per second for the following cases:

(a) Compressor pressure ratio chosen to give maximum thp/M_a ($X=1$)

(b) Compressor pressure ratio chosen to give minimum W_f/thp

At each flight speed, the corresponding optimum jet velocity is used.

This figure shows that t_0 has an important effect on the performance values; the thp/M_a decreases and the specific fuel consumption increases appreciably as t_0 increases. For the given conditions, the thp/M_a decreases about 30 percent for both cases (a) and (b) as t_0 increases from 393° to 519° R (the 393° R temperature corresponds to an NACA standard altitude of 35,332 ft, the start of the tropopause). The values of thp/M_a for case (a) are about 13 percent greater than those for case (b) over the range of t_0 investigated.

The specific fuel consumption increases about 25 percent for both cases (a) and (b) as the ambient-air temperature increases from 393° to 519° R. The values of W_f/thp for case (a) are about 10 percent higher than those for case (b). It is also evident from figure 9 that increasing flight speed results in only slightly increased values of thp/M_a and slightly decreased values of W_f/thp for both cases (a) and (b). Over the range of ambient-air temperatures considered, increasing the flight speed from 367 to 733 feet per second results in changes in thp/M_a and W_f/thp of about 2 percent.

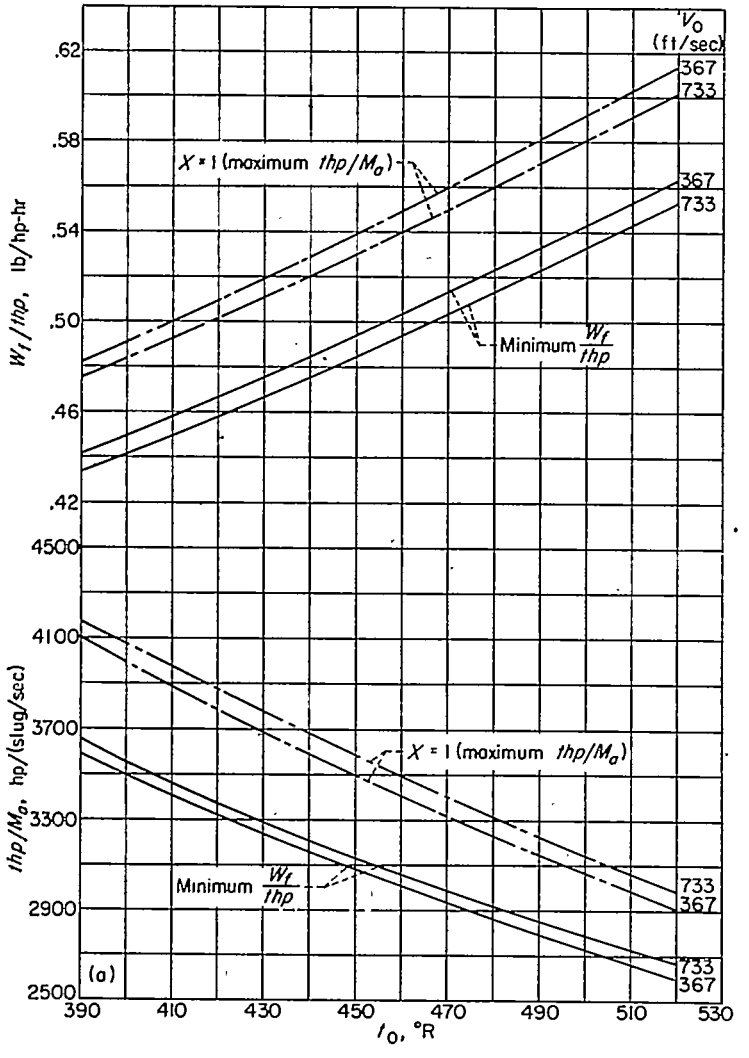

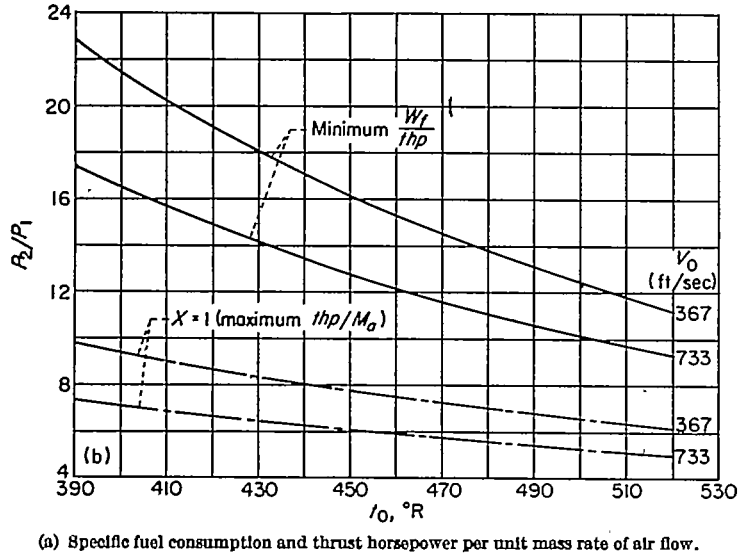

(a) Specific fuel consumption and thrust horsepower per unit mass rate of air flow.

(b) Compressor pressure ratios for minimum $\frac{W_f}{thp}$ and $X=1$.

FIGURE 9.—Effects of flight speed and ambient-air temperature on performance at compressor pressure ratios for minimum specific fuel consumption and for maximum thrust horsepower per unit mass rate of air flow; T_t, 1960° R; η_c, 0.85; η_t, 0.90; η_p, 0.85; η_b, 0.96; C_t, 0.97; h, 18,900 Btu per pound; ϵ, 1.00.

The compressor pressure ratios associated with the performance values given in figure 9 (a) are presented in figure 9 (b). The large increase in required pressure ratio from the condition of $X=1$ to the condition of minimum specific fuel consumption is to be noted.

In figures 8 and 9, it was assumed that the compressor adiabatic efficiency remains constant at 0.85 regardless of the pressure ratio. As the desired pressure ratio is increased, however, it becomes increasingly difficult to design a compressor to maintain a high adiabatic efficiency. A reduction in the compressor adiabatic efficiency with increase in pressure ratio reduces the gains derived from increase in pressure ratio and hence reduces the value of the optimum pressure ratios for maximum thrust horsepower per unit mass rate of air flow and for minimum specific fuel consumption.

This condition is illustrated in figure 10 in which a turbine-propeller engine equipped with a multistage axial-flow compressor having a polytropic efficiency $\eta_{c,p}$ of 0.88 is considered. The other parameters of the engine are the same

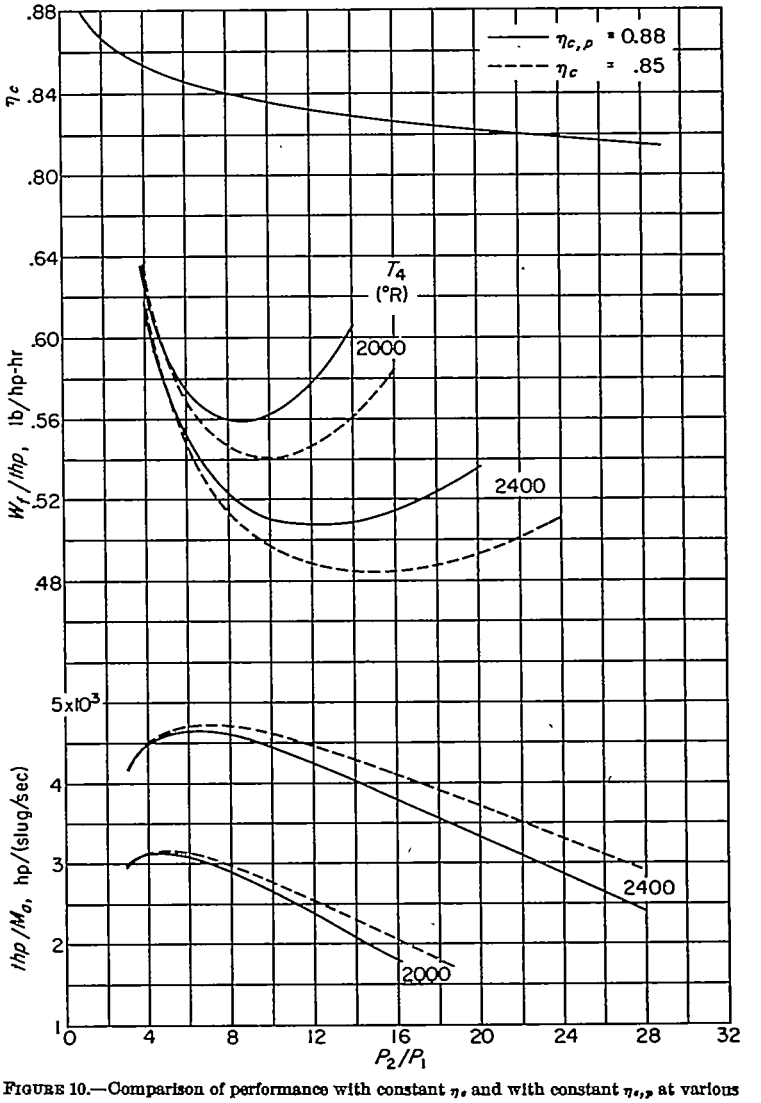

FIGURE 10.—Comparison of performance with constant η_c and with constant $\eta_{c,p}$ at various compressor pressure ratios; V_0, 733 feet per second; V_j, 902 feet per second; t_0, 519° R; η_p, 0.85; η_t, 0.90; η_b, 0.96; C_t, 0.97; h, 16,900 Btu per pound; ϵ, 1.00.

as for figure 8 (b). Figure 10 shows the over-all adiabatic efficiency of the compressor, the specific fuel consumption, and the thrust horsepower per unit mass rate of air flow for a range of pressure ratios. The pressure ratio is increased by adding stages to the compressor. Although the polytropic efficiency is held constant, the over-all compressor adiabatic efficiency decreases with increase in pressure ratio. At a pressure ratio of 5, the compressor adiabatic efficiency is 0.85, the value used in the computations for figures 8 and 9. For the range of T_4 shown, the values of P_2/P_1 for maximum thp/M_a and minimum W_f/thp are lower for the case when the reduction in compressor adiabatic efficiency with increased pressure ratio is considered than those for the case of constant η_c of 0.85. This change in P_2/P_1 for maximum thp/M_a and minimum W_f/thp is more pronounced at the higher value of T_4.

The effect of increasing pressure ratio across the turbine on turbine efficiency is not easily predicted. In the design of a turbine for greater pressure ratios, the number of turbine stages is usually increased and the pressure ratio per stage is increased, in order to economize on the size and weight of the turbine. Increasing the number of turbine stages tends to improve the over-all turbine efficiency (provided that the efficiency per stage remains the same). However, increasing the pressure ratio per stage may result in some reduction in stage efficiency, which will offset the gains obtained by the increased number of stages. The net effect on the over-all turbine efficiency depends on the compromise between pressure ratio per stage and number of stages.

ENGINE WITH GIVEN SET OF MATCHED COMPONENTS

The points on the previous performance curves pertain to a series of turbine-propeller engines in which the components are changed to provide the desired characteristics at each point. It is of interest to examine over a variety of operating conditions the characteristics of a turbine-propeller engine having given components.

Two engines are considered in this study. One engine has a propeller, an axial-flow compressor, and two independent turbines (divided turbine system); one turbine drives only the compressor and the other drives only the propeller. The second engine contains the same components, except that the two turbines are connected to provide a single rotating system (connected turbine system). Components chosen have performance characteristics fairly representative of their type and are not to be interpreted as being the best available. Although the performance of each engine depends on the characteristics of the particular components chosen, some general trends may be demonstrated by considering the illustrative case. Plots of the characteristics of the components and the performance of the turbine-propeller engines incorporating these components are presented in figures 11 to 18. Calculations of engine performance were simplified by neglecting the mass of fuel in evaluating turbine output, by neglecting any losses in transmitting the shaft power from turbine to propeller, and by assuming the drop in total pressure through the combustion chamber proportional to the combustion-chamber-inlet total pressure. The errors introduced by these simplifications are too small to influence the basic trends illustrated. In the computation of the performance of the turbine-propeller engine, the following parameters are assumed:

Combustion efficiency, η_b	0.96
Exhaust-nozzle velocity coefficient, C_v	0.97
Lower heating value of fuel, h, Btu/lb	18,000

In order to simplify the specific fuel consumption plots, the specific heat at constant pressure of the gases during combustion was assumed to be a function only of T_4/T_1.

Compressor characteristics.—The conventional presentation of the performance curves for an illustrative 8-stage axial-flow compressor is given in figure 11. Values of P_2/P_1, η_c, and K_c are plotted against the $M_a\sqrt{\theta_1}/\delta_1$ for various values of $U_c/\sqrt{\theta_1}$. The slip factor is defined as

$$K_c=\frac{550\,hp_c}{M_aU_c^2} \tag{10}$$

At a given $U_c/\sqrt{\theta_1}$, reducing the $M_a\sqrt{\theta_1}/\delta_1$ by throttling the compressor outlet first results in a very rapid increase in pressure ratio and efficiency and then a more gradual increase in these parameters to peak values. Excessive throttling to the position indicated by the surge line results

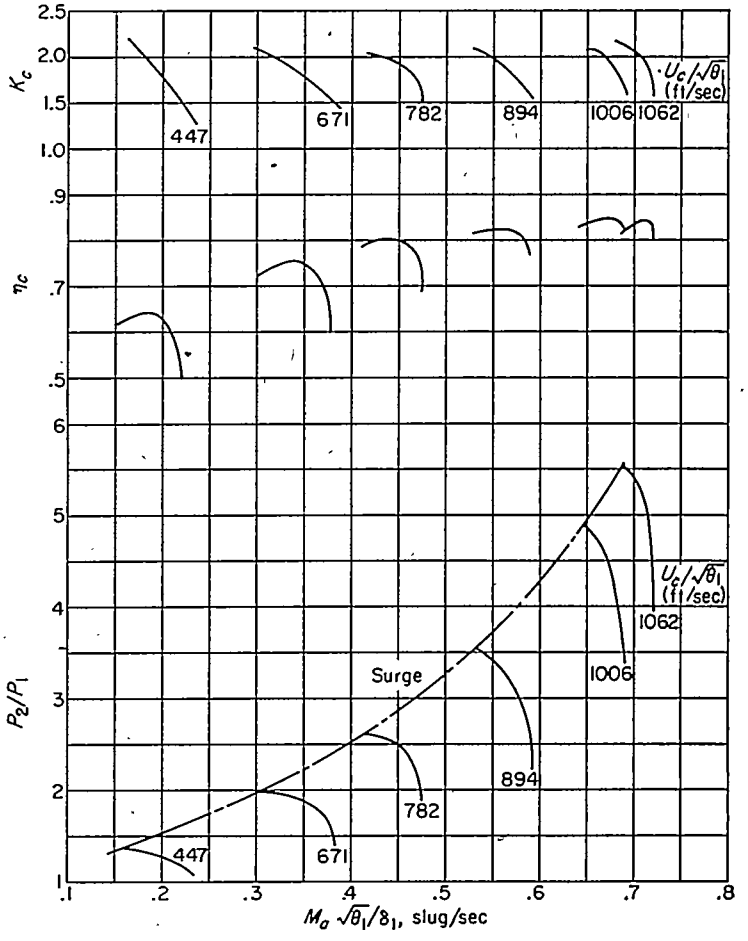

FIGURE 11.—Characteristics of axial-flow compressor.

in stalling of the compressor, which is accompanied by surging of the air flow. It is to be noted that operation at higher tip speeds is limited to narrower ranges of mass flow.

Turbine characteristics.—The performance characteristics of a typical single-stage turbine with moderate reaction are shown in figure 12. The mass-flow factor of the gas through the turbine is plotted in figure 12 (a) against P_4/p_5 for various values of $U_{t,1}/V_{t,1}$. The turbine jet velocity $V_{t,1}$ is defined as the theoretical jet velocity developed by the gas expanding isentropically through the turbine nozzle from turbine-inlet total temperature and pressure to turbine-outlet static pressure. The values of the upper abscissa $V_{t,1}/\sqrt{\theta_4}$ corresponding to the values of P_4/p_5 are obtained from the velocity equation

$$\frac{V_{t,1}}{\sqrt{\theta_4}}=\sqrt{2Jc_{p,g}519\left[1-\left(\frac{p_5}{P_4}\right)^{\frac{\gamma_g-1}{\gamma_g}}\right]}$$

The values of the upper ordinate $M_gV_{t,1}/\delta_4$ are obtained from the product of $M_g\sqrt{\theta_4}/\delta_4$ and $V_{t,1}/\sqrt{\theta_4}$. For pressure ratios across the turbine greater than 2.54, the value of $M_g\sqrt{\theta_4}/\delta_4$ is constant (that is, choking occurs at the turbine nozzle).

The turbine total efficiency $\eta_{t,1}$ is principally a function of $U_{t,1}/V_{t,1}$ and, to a lesser extent, a function of the pressure ratio across the turbine and the Reynolds number; $\eta_{t,1}$ is defined as

$$\eta_{t,1}=\frac{550\,hp_{t,1}}{\frac{M_g}{2}V_{t,1}^2-\frac{M_g}{2}V_5^2} \qquad (11a)$$

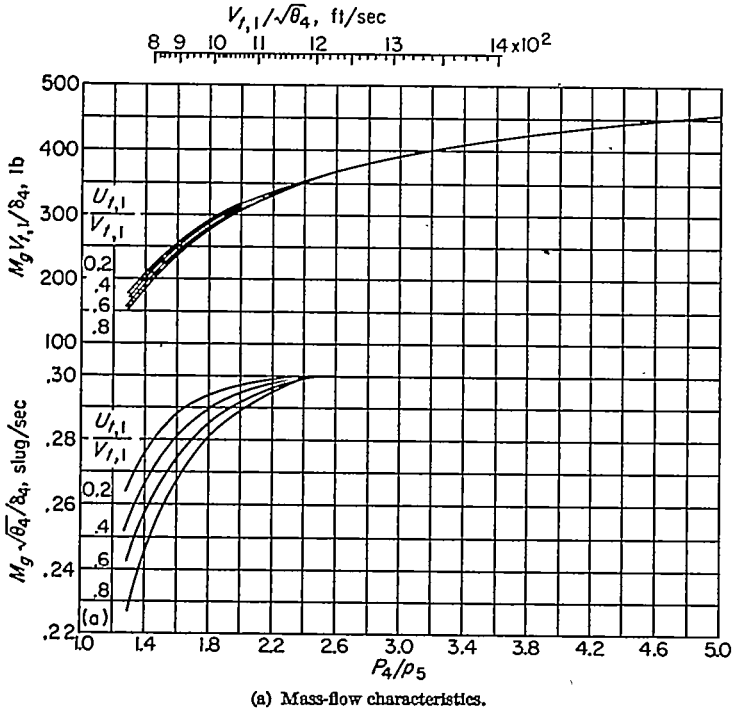

(a) Mass-flow characteristics.

FIGURE 12.—Characteristics of first single-stage turbine.

The relation between total efficiency, blade-to-jet speed ratio, and pressure ratio is given in figure 12 (b); the Reynolds number effect is omitted in this analysis. The turbine-shaft efficiency $\eta'_{t,1}$, also shown in figure 12 (b), is defined as

$$\eta'_{t,1}=\frac{550\,hp_{t,1}}{\frac{1}{2}M_gV_{t,1}^2} \qquad (11b)$$

In this definition the turbine is not credited with kinetic power corresponding to the average axial velocity of the gas at the turbine discharge. In the plot of $\frac{\sqrt{\eta'_{t,1}}}{U_{t,1}/V_{t,1}}$ against $U_{t,1}/V_{t,1}$ in figure 12 (b), the effect of P_4/p_5 is so slight that only a single curve is shown. The parameters $\frac{\sqrt{\eta'_{t,1}}}{U_{t,1}/V_{t,1}}$ and $M_gV_{t,1}/\delta_4$ are useful in evaluating turbine operating conditions for given turbine work output and compressor operating conditions.

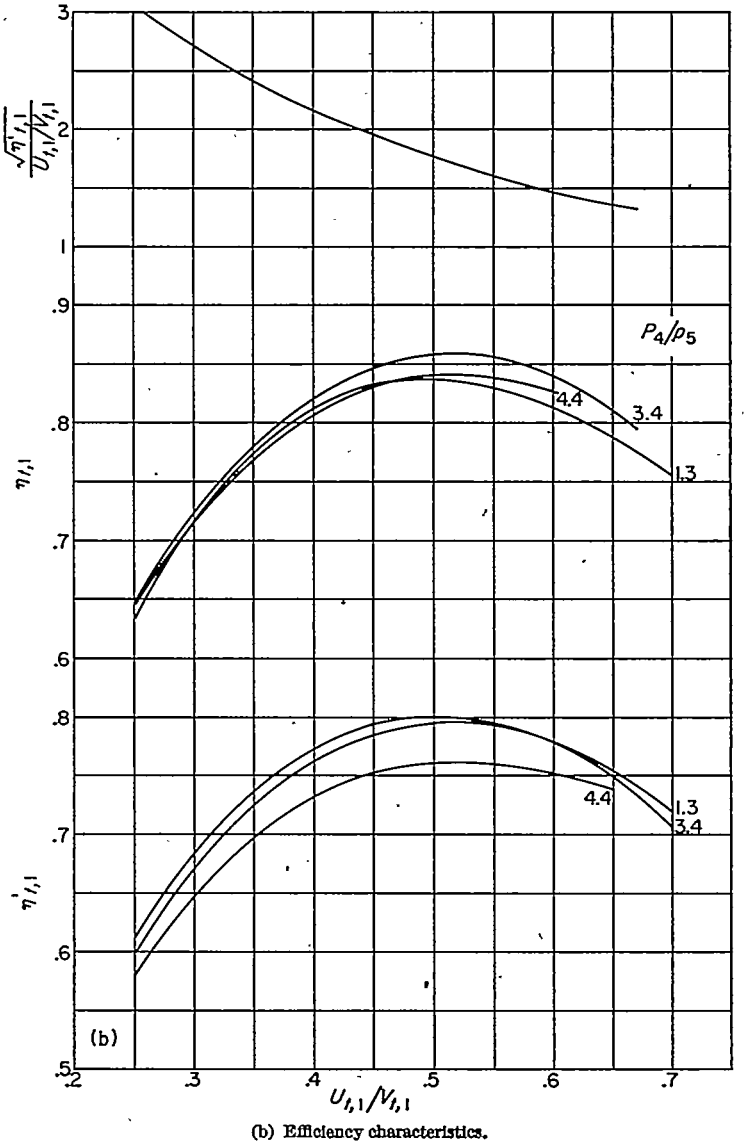

(b) Efficiency characteristics.

FIGURE 12.—Concluded. Characteistics of first single-stage turbine.

Gas generator.—The combination of compressor, combustor, and turbine which drives the compressor is referred to as the gas generator. It converts the heat energy from the fuel to energy available in high-temperature, pressurized gases. These gases are expanded in a second turbine which drives the propeller and are further expanded in the exhaust nozzle to provide jet power.

When the compressor and the turbine of the gas generator are matched, it is necessary that the mass flows through the components be consistent (that is, the gas flow through the turbine equal the sum of the air flow through the compressor and the fuel flow) and that the compressor work required equal the turbine work output. The compressor and the turbine sizes are so adjusted that desired mass-flow factors through the components are obtained when the compressor is operating at its design point and design turbine-inlet to compressor-inlet temperature ratio T_4/T_1 is maintained. The turbine of figure 12 is matched with the compressor of figure 11 for a design-point temperature ratio T_4/T_1 of 4.23 and a design compressor pressure ratio P_2/P_1 of 5.1 at a tip speed factor $U_c/\sqrt{\theta_1}$ of 1062 feet per second. These conditions permit operation sufficiently far from the compressor surge line to ensure stable operation of the gas generator over a wide range of conditions off the design point.

Lines of constant temperature ratio T_4/T_1 for the matched turbine and compressor are shown superimposed on compressor characteristics in figure 13 (a). If the difference between M_a and M_g (due to added fuel) is neglected, the following identity can be written:

$$\frac{M_a\sqrt{T_1}}{P_1}=\frac{P_4}{P_1}\sqrt{\frac{T_1}{T_4}}\frac{M_g\sqrt{T_4}}{P_4}$$

If r represents the ratio of the drop in combustion-chamber total pressure to the compressor-outlet total pressure, then

$$\Delta P_2=P_2-P_4=rP_2$$

or

$$P_4=(1-r)P_2$$

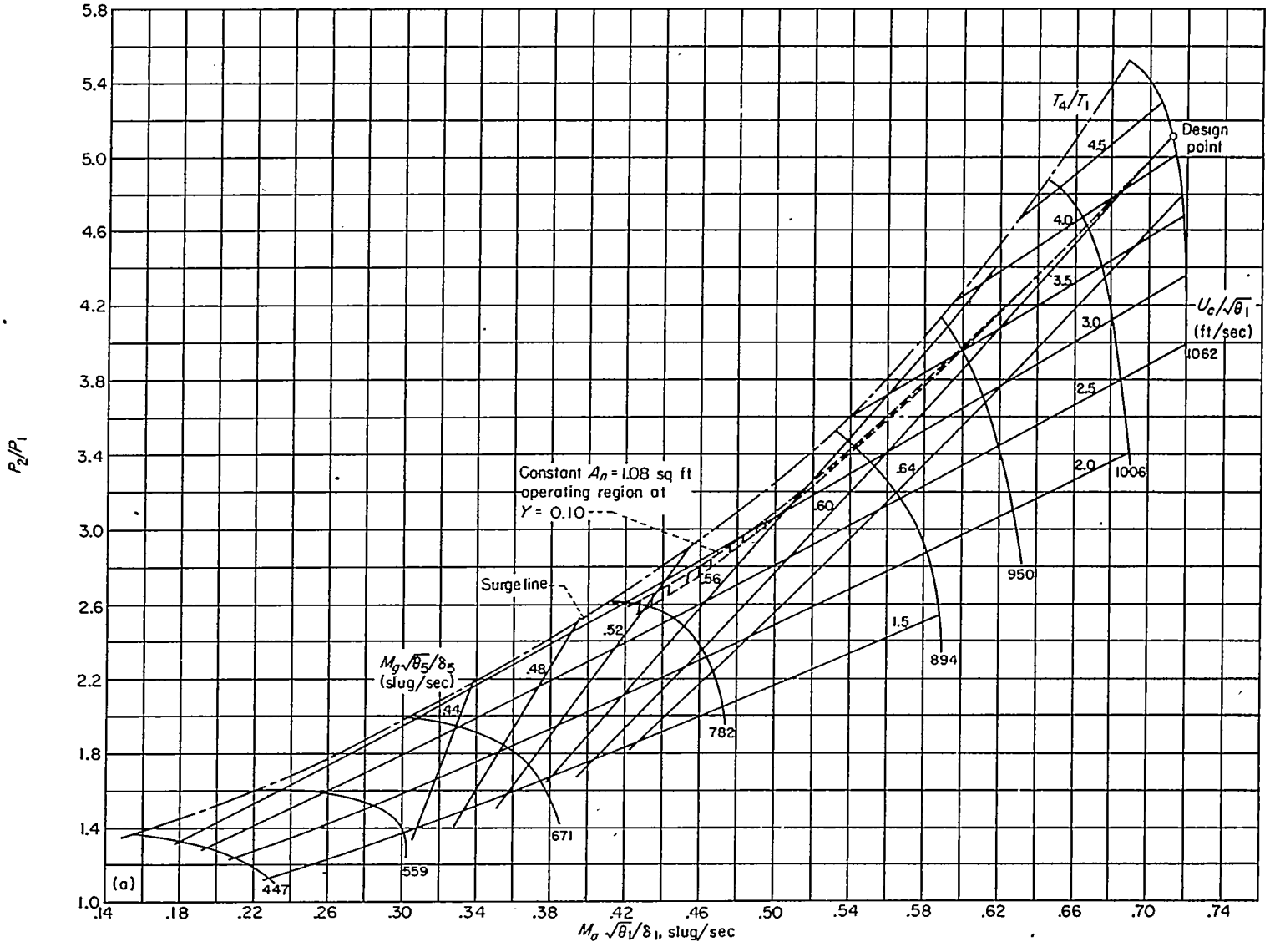

(a) Lines of constant T_4/T_1 and constant $M_g\sqrt{\theta_5}/\delta_5$.

FIGURE 13.—Operating characteristics of gas generator consisting of matched compressor and turbine which drives compressor; $\Delta P_2/P_2$, 0.05; U_c/U_{t1}, 1.0.

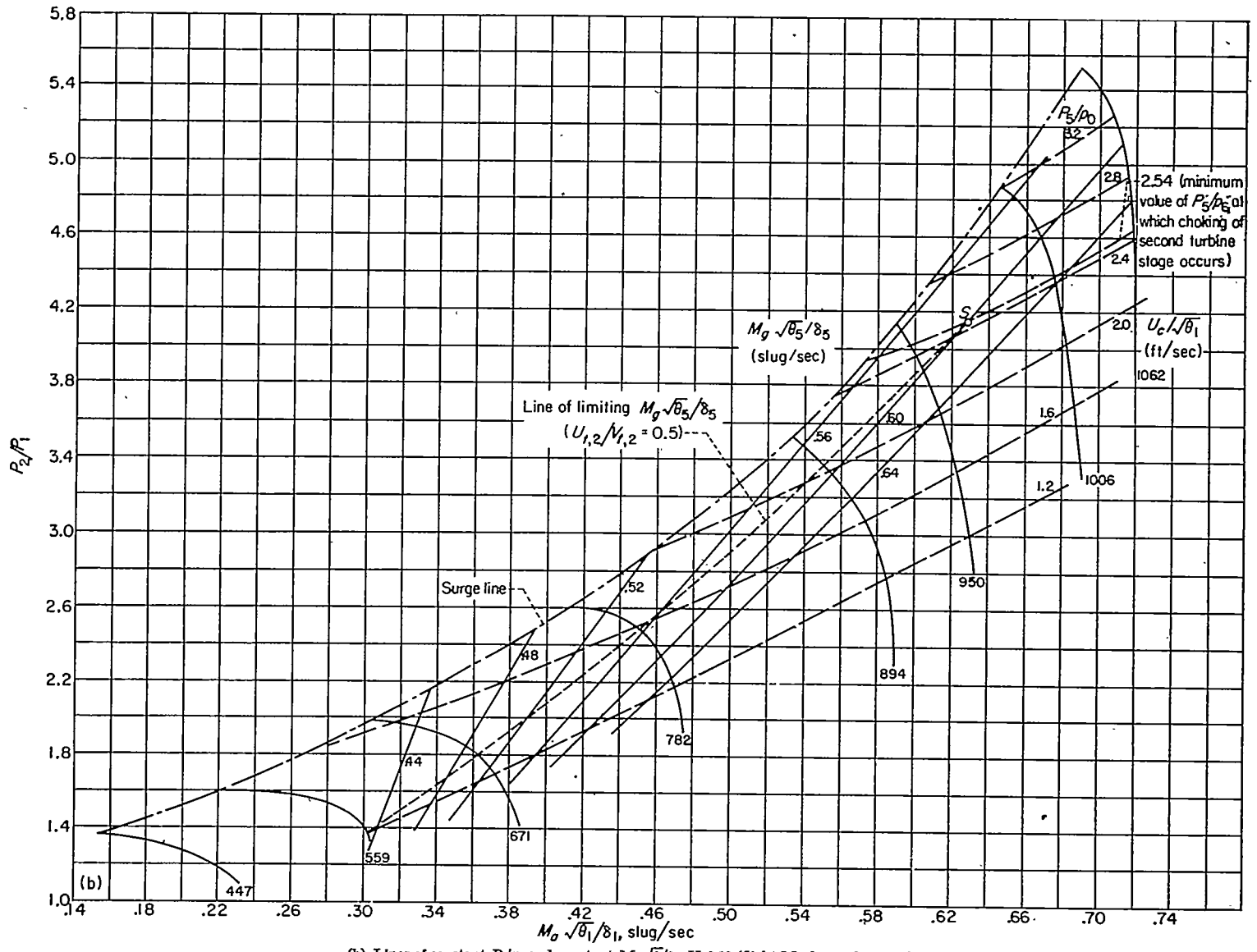

(b) Lines of constant P_4/p_0 and constant $M_g\sqrt{\theta_5}/\delta_5$; Y, 0.10 (flight Mach number, 0.71).

FIGURE 13.—Continued. Operating characteristics of gas generator consisting of matched compressor and turbine which drives compressor; $\Delta P_2/P_2$, 0.05; $U_c/U_{1,1}$, 1.0.

Hence,

$$\frac{M_a\sqrt{T_1}}{P_1}=(1-r)\frac{P_2}{P_1}\sqrt{\frac{T_1}{T_4}}\frac{M_a\sqrt{T_4}}{P_4}$$

or

$$\frac{M_a\sqrt{\theta_1}}{\delta_1}=(1-r)\frac{P_2}{P_1}\sqrt{\frac{T_1}{T_4}}\frac{M_g\sqrt{\theta_4}}{\delta_4} \tag{12}$$

In operating regions where choking of the flow occurs at the turbine nozzle, the value of $M_g\sqrt{\theta_4}/\delta_4$ becomes constant (for example, for pressure ratios P_4/p_5 greater than 2.54 for the turbine shown in fig. 12 (a)). When this constant value of $M_g\sqrt{\theta_4}/\delta_4$ is substituted into equation (12) and a value is assumed for r, it is possible to compute the value T_4/T_1 at any value of $M_a\sqrt{\theta_1}/\delta_1$ and the corresponding P_2/P_1. In the nonchoking region, the value of $M_g\sqrt{\theta_4}/\delta_4$ is not so easily determined, and the more general method described in appendix C is used.

It is evident from the lines of constant T_4/T_1 that, at any given rotational speed and compressor-inlet temperature T_1, increasing the combustion-chamber-outlet temperature T_4 is equivalent to throttling the compressor. This increase in T_4 causes an increase in compressor pressure ratio and decreases the mass-flow factor. Excessive combustion-chamber-outlet temperature may carry operation into the surge zone.

Lines of constant $M_g\sqrt{\theta_5}/\delta_5$ are also plotted on the gas-generator operating curves (fig. 13) because these curves link the operation of the second turbine with that of the gas generator. If the difference between M_a and M_g is again neglected, the following identity can be written:

$$\frac{M_g\sqrt{\theta_5}}{\delta_5}=\frac{M_a\sqrt{\theta_1}}{\delta_1}\sqrt{\frac{T_5}{T_4}\frac{T_4}{T_1}}\left(\frac{P_1}{P_4}\frac{P_4}{P_5}\right) \tag{13}$$

At any operating point, the quantities $M_a\sqrt{\theta_1}/\delta_1$, T_4/T_1, and P_2/P_1 can be read and P_4/P_1 computed from

$$P_4/P_1=(1-r)P_2/P_1$$

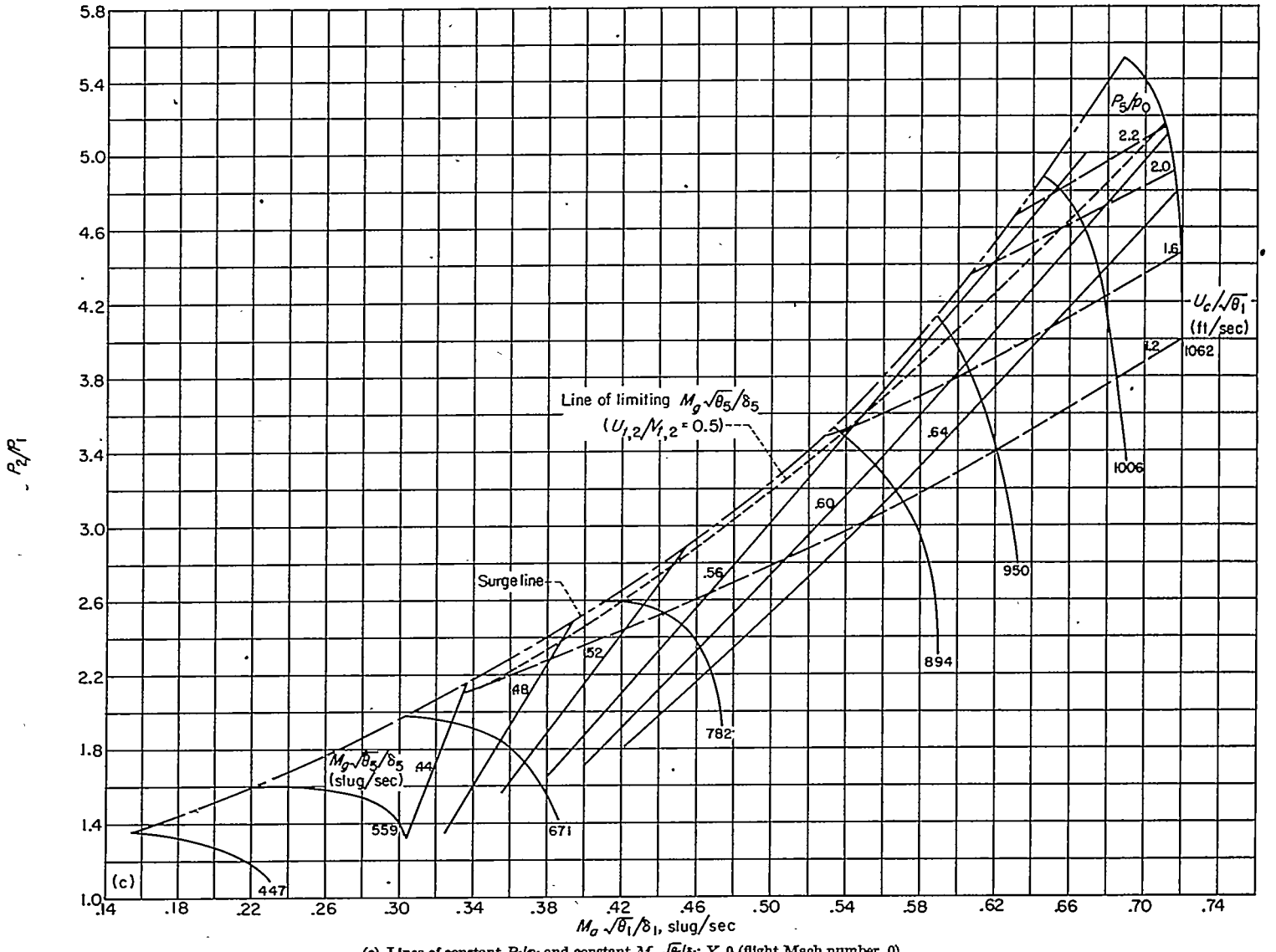

(c) Lines of constant P_5/p_0 and constant $M_g\sqrt{\theta_5}/\delta_5$; Y, 0 (flight Mach number, 0).

FIGURE 13.—Concluded. Operating characteristics of gas generator consisting of matched compressor and turbine which drives compressor; $\Delta P_2/P_2$, 0.05; $U_c/U_{t,1}$, 1.0.

The corresponding values of P_4/P_5 and T_5/T_4 are determined by the method described in appendix C, and the corresponding $M_g\sqrt{\theta_5}/\delta_5$ is evaluated from equation (13).

For the gas-generator combination, the compressor power is equal to the turbine power; hence, from equations (10) and (11) and again from the assumption that M_a and M_g are equal,

$$K_c U_c^2 = \frac{1}{2}\eta'_{t,1} V_{t,1}^2 \tag{14}$$

and

$$K_c\left(\frac{U_c}{U_{t,1}}\right)^2 = \frac{1}{2}\left(\frac{V_{t,1}}{U_{t,1}}\right)^2 \eta'_{t,1} \tag{15}$$

The ratio of compressor tip speed U_c to the turbine-blade speed $U_{t,1}$ is a constant for any given engine. Thus, any value of K_c determines the value of $\eta'_{t,1}(V_{t,1}/U_{t,1})^2$ and, from figure 12 (b), determines the value of $U_{t,1}/V_{t,1}$ from which the values of $\eta_{t,1}$ and $\eta'_{t,1}$ can be obtained, when the effect of pressure ratio across the turbine is neglected. A value of $U_c/U_{t,1}$ equal to 1.0 was chosen for the engine. For the compressor shown in figure 11, the variation in the value of K_c over the entire operating range was from 1.5 to 2.1. The corresponding variation in $U_{t,1}/V_{t,1}$ was small enough that the turbine operated at nearly constant efficiency over the entire operating range of the gas generator.

Matching second turbine.—For operation at a given flight Mach number, a characteristic of the gas generator is that along a given $U_c/\sqrt{\theta_1}$ line the pressure ratio available for further expansion at the inlet to the second turbine P_5/p_0 decreases as $M_g\sqrt{\theta_5}/\delta_5$ increases. This trend is shown in figures 13 (b) (for $Y=0.10$) and 13 (c) (for $Y=0$), which are plots of the gas-generator operating characteristics showing lines of $M_g\sqrt{\theta_5}/\delta_5$ (which are independent of flight speed) and lines of P_5/p_0 (which are a function of flight speed). The possible operating range on figure 13 is located between the surge line and the line of limiting values of $M_g\sqrt{\theta_5}/\delta_5$ permitted

by the second turbine. Any limiting value of $M_g\sqrt{\theta_5}/\delta_5$ is the value of the mass-flow factor through the second turbine when the pressure ratio across the turbine is equal to the maximum pressure ratio available P_5/p_0. It is evident that the second turbine should be designed to permit limiting values of $M_g\sqrt{\theta_5}/\delta_5$ sufficiently large to provide the engine with a reasonable range of operation on the gas-generator plot. The increase in $M_g\sqrt{\theta_5}/\delta_5$ is accomplished by designing a larger second-turbine nozzle area. Excessive increase in design turbine-nozzle area should be avoided, however, because, for a given $M_g\sqrt{\theta_5}/\delta_5$ (as set by the gas generator), there results a reduction in pressure ratio required across the second turbine, which is accompanied by a reduction in the power obtainable from this turbine. An inefficient distribution of power between the propeller and the exhaust jet may result. The second-turbine nozzle area chosen for design operating conditions should be the best compromise between extent of operation and efficiency of power distribution between the propeller and the exhaust jet.

The characteristics of the second turbine which drives the propeller are shown in figure 14. They are similar to those of the turbine driving the compressor (fig. 12), except that the maximum values of the mass-flow factor are different.

Matching propeller.—The problem of propeller matching involves mainly the selection of proper propeller size and proper relation between propeller and turbine speeds, so that the propeller will have a high efficiency at engine design conditions and maintain high efficiency over a wide range of off-design engine operation. A value of $U_{t,2}/N_p$, based on reasonable estimates of turbine pitch-line diameter and gear reduction ratio between the turbine and the propeller, is chosen. This value of $U_{t,2}/N_p$, when once fixed for a given engine, determines the value of $N_p/\sqrt{\theta_1}$ for any engine operating condition ($U_{t,2}/V_{t,2}$ and $V_{t,2}/\sqrt{\theta_1}$ being known for that operating condition) and affects the manner in which propeller efficiency varies with changing engine operating conditions. At any operating condition of the engine, the flight speed factor $V_0/\sqrt{\theta_1}$ is known, and the propeller-shaft horsepower factor $hp_p/\sqrt{\theta_1}\delta_1$ can be evaluated. Fixing the values of propeller diameter D_p and $U_{t,2}/N_p$ (and hence, $N_p/\sqrt{\theta_1}$) determines the values of power coefficient C_p and advance ratio V_0/N_pD_p at every operating point; these values in turn determine the propeller efficiency. The variation of propeller efficiency with engine operating conditions depends on the values of D_p and $U_{t,2}/N_2$ selected. Therefore, the propeller diameter D_p and, to some extent, the value of $U_{t,2}/N_p$ are adjusted by trial until a good compromise of propeller efficiency and engine operating range is obtained. Reference 6 presents a similar and more detailed discussion of matching a propeller to a turbine for the same type engine considered here. Figure 15 shows the characteristics of a high-efficiency four-bladed propeller at flight Mach numbers of 0.55 and 0.71. Values of the power coefficient C_p are plotted against the advance ratio V_0/N_pD_p for various values of propeller efficiency and blade angle. The propeller efficiency is largely dependent on tip Mach number and drops off rapidly when a value of tip Mach number slightly greater than 1 is exceeded. The maximum efficiencies range from

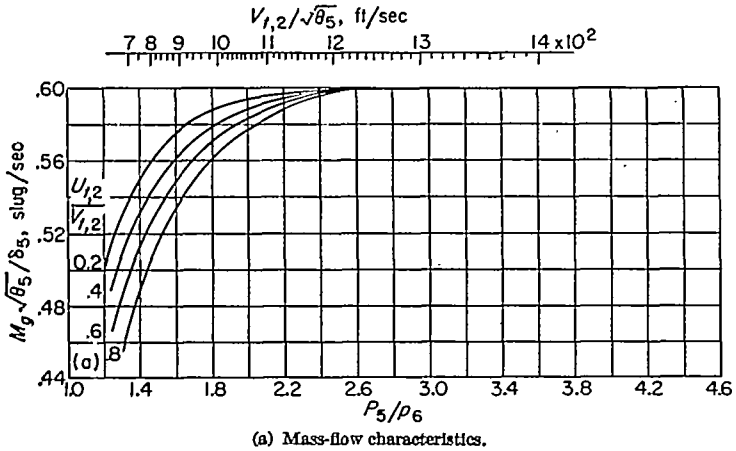

(a) Mass-flow characteristics.

FIGURE 14.—Characteristics of second single-stage turbine.

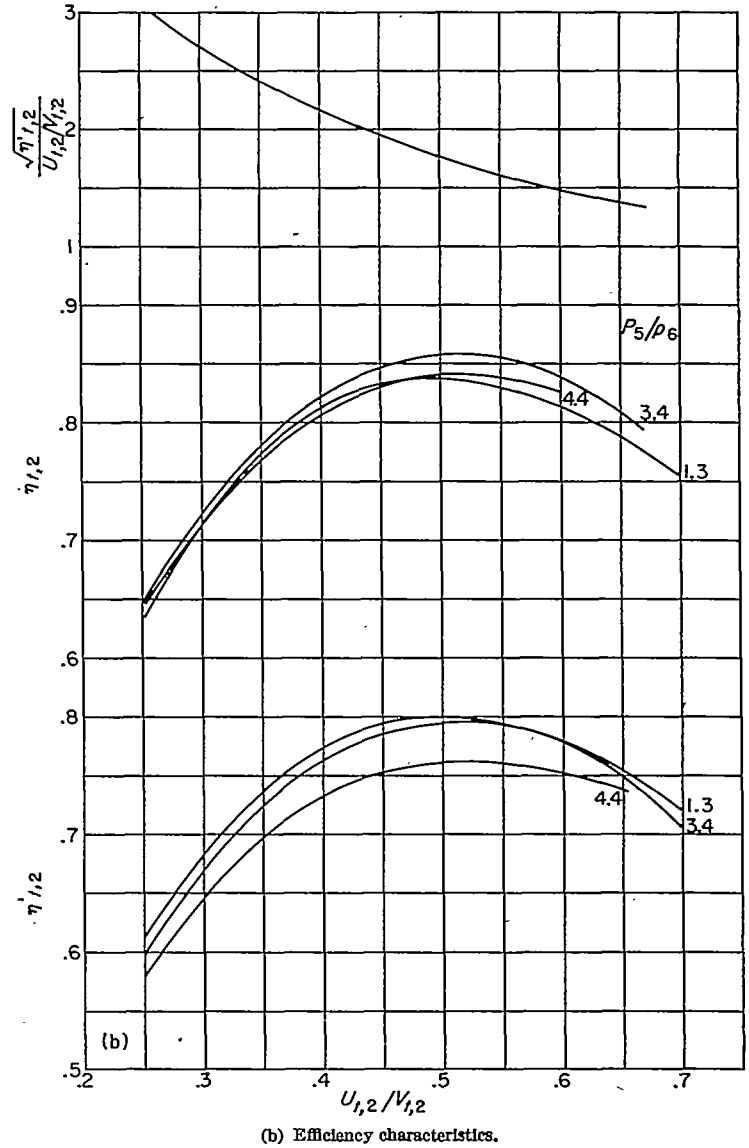

(b) Efficiency characteristics.

FIGURE 14.—Concluded. Characteristics of second single-stage turbine.

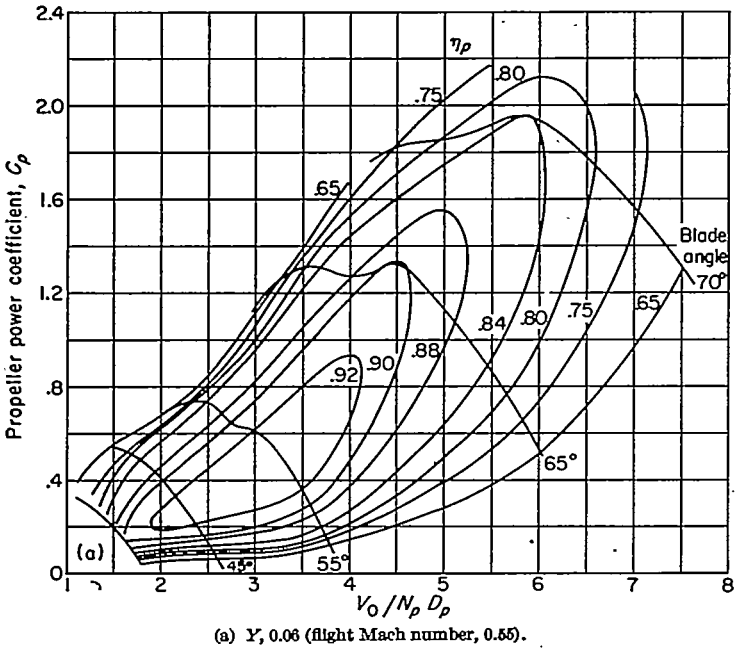

(a) Y, 0.06 (flight Mach number, 0.55).

FIGURE 15.—Characteristics of high-speed propeller.

about 0.93 at flight Mach number of 0.55 to about 0.88 at flight Mach number of 0.71. At higher flight Mach numbers, because tip Mach numbers greater than 1 are almost always encountered, lower efficiencies exist. The values of propeller efficiency presented in figure 15 are based on actual shaft power input to the propeller and do not include losses involved in the transmission of power from turbine to propeller.

Performance of engine with divided turbine system.—Any point on the plot in figure 13 (a) represents the gas generator operating at a given set of conditions such as $U_c/\sqrt{\theta_1}$, $M_a\sqrt{\theta_1}/\delta_1$, T_4/T_1, P_2/P_1, and $M_g\sqrt{\theta_5}/\delta_5$. The $M_g\sqrt{\theta_5}/\delta_5$ at any point is fixed; it is therefore evident from figure 14 (a) that the second turbine, if unchoked, can operate only over a range of definite combinations of $U_{t,2}/V_{t,2}$ and P_5/p_6. Hence, for every point on the gas-generator curve the second turbine can operate over an extent of pressure ratio P_5/p_6 and corresponding $U_{t,2}/V_{t,2}$; the power output of the turbine, the turbine efficiency, the jet power of the engine, the propeller speed, and the propeller efficiency all vary accordingly.

When the mass-flow factor $M_g\sqrt{\theta_5}/\delta_5$ is the maximum value that the second turbine can attain (in other words the flow through the turbine is choked), the pressure ratio across the turbine is independent of $U_{t,2}/V_{t,2}$ (see fig. 14 (a)). Thus any point on the gas-generator plot along this choking $M_g\sqrt{\theta_5}/\delta_5$ line corresponds to operation at any combination of $U_{t,2}/V_{t,2}$ and P_5/p_6. (The quantity P_5/p_6 may have any value equal to or greater than that required for choking but not appreciably greater than the available P_5/p_0 at the operating point. The case in which p_6 is less than p_0 is possible; however, it necessitates a diffuser to discharge the gas from the turbine outlet to the atmosphere and is generally not a desirable condition.)

The value of $M_g\sqrt{\theta_5}/\delta_5$ which gives choked flow in the second turbine sets one of the limits on the possible operating region in figure 13 (a). For the turbine under consideration (fig. 14), the maximum value of $M_g\sqrt{\theta_5}/\delta_5$ is 0.60 slug per second, and hence all points in figure 13 (a) at values of $M_g\sqrt{\theta_5}/\delta_5$ greater than 0.60 slug per second are unattainable. Furthermore, in order to attain this choked flow, the available P_5/p_0 must be equal to or greater than the choking pressure ratio 2.54 given in figure 14 (a). Figure 13 (b) shows the pressure ratios P_5/p_0 corresponding to figure 13 (a) and $Y=0.10$ (Mach number, 0.71). The point S marks the intersection of the line of $M_g\sqrt{\theta_5}/\delta_5=0.60$ slug per second with the line of $P_5/p_0=2.54$. All points on the line of $M_g\sqrt{\theta_5}/\delta_5=0.60$ slug per second to the right of point S have values of P_5/p_0 greater than 2.54 and hence are attainable conditions.

To the left of point S in figure 13 (b), the line of $M_g\sqrt{\theta_5}/\delta_5=$ 0.60 slug per second intersects values of P_5/p_0 less than 2.54 and hence is an unattainable condition (if p_6 is limited to values equal to or greater than p_0). Figure 14 (a) indicates that in this region the attainable value of $M_g\sqrt{\theta_5}/\delta_5$ depends on the values of P_5/p_6 and $U_{t,2}/V_{t,2}$. The dashed curve in figure 13 (b) gives the maximum attainable value of $M_g\sqrt{\theta_5}/\delta_5$ corresponding to the condition $U_{t,2}/V_{t,2}=0.5$ (at which the efficiency of the second turbine is a maximum). The region in figure 13 (b) between the line of maximum attainable $M_g\sqrt{\theta_5}/\delta_5$ and the surge line is the possible operating range for the combination of turbines chosen in this illustration at $Y=0.10$. The dashed curve can be shifted somewhat by choosing a different value of $U_{t,2}/V_{t,2}$.

The conditions of figure 13 (c) correspond to those of figure 13 (a) and zero flight speed ($Y=0$). In this case all values of

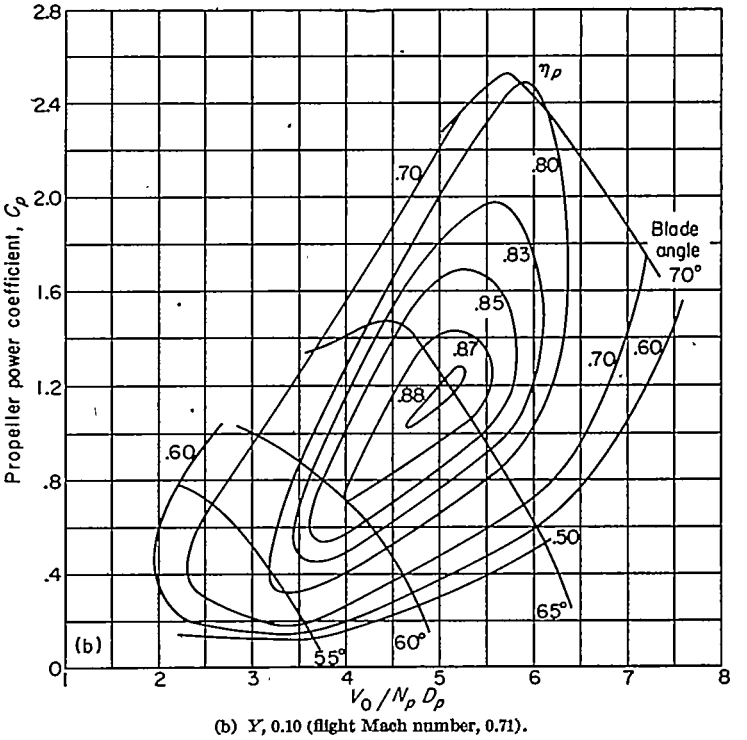

(b) Y, 0.10 (flight Mach number, 0.71).

FIGURE 15.—Concluded. Characteristics of high-speed propeller.

P_5/p_0 shown are less than 2.54, and the choked condition in the second turbine is not attained. The dashed curve is again the upper limit on the value of $M_g\sqrt{\theta_5}/\delta_5$ for $U_{t,2}/V_{t,2}=0.50$, and operation for this flight condition is limited to the narrow strip between the dashed line and the surge line.

The permissible operational region discussed in connection with figure 13 will now be discussed in greater detail.

A plot showing the relation between operating parameters of the second turbine and the gas generator is shown in figure 16. The blade-to-jet speed ratio $U_{t,2}/V_{t,2}$ is plotted against P_5/p_6 for lines of constant T_4/T_1 or $M_a\sqrt{\theta_1}/\delta_1$. Figure 16 (a) is for a constant tip-speed factor of 1062 feet per second. Every point on the gas-generator plot (fig. 13) at this value of tip-speed factor has a unique value of $M_a\sqrt{\theta_1}/\delta_1$ and T_4/T_1 and is represented by a line of operation on the engine operating plot of figure 16 (a). This characteristic is evident from the previous discussion, in which it was shown that there is a series of combinations of $U_{t,2}/V_{t,2}$ and P_5/p_6 corresponding to every point on the gas-generator plot. The region in figure 16 (a) at pressure ratios P_5/p_6 of 2.54 and greater (in which the second turbine is choked) corresponds to operation at the point in figure 13 on the $U_d/\sqrt{\theta_1}=1062$ feet per second line where $M_g\sqrt{\theta_5}/\delta_5=0.60$ slug per second.

The operation-limit lines at which the entire P_5/p_0 available equals P_5/p_6, for flight Mach numbers equal to 0 ($Y=0$), 0.55 ($Y=0.06$), and 0.71 ($Y=0.10$), are also shown on figure 16 (a); operation is possible between the surge line and these limit lines for the specified Mach number. It is noted that for zero flight speed ($Y=0$) the P_5/p_0 available is never great enough to obtain choked flow through the second turbine. Figure 16 (b) is similar to figure 16 (a), except that the compressor tip-speed factor is 1006 feet per second. Because the available P_5/p_0 is lower at this lower $U_d/\sqrt{\theta_1}$, the range of operation of the turbine at the same flight Mach numbers is smaller.

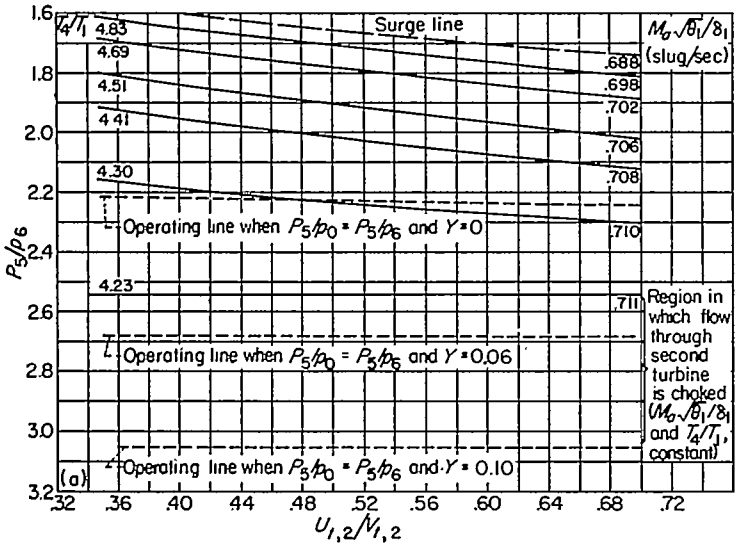

(a) $U_d/\sqrt{\theta_1}$, 1062 feet per second.

FIGURE 16.—Relation between operating parameters of second turbine and gas generator.

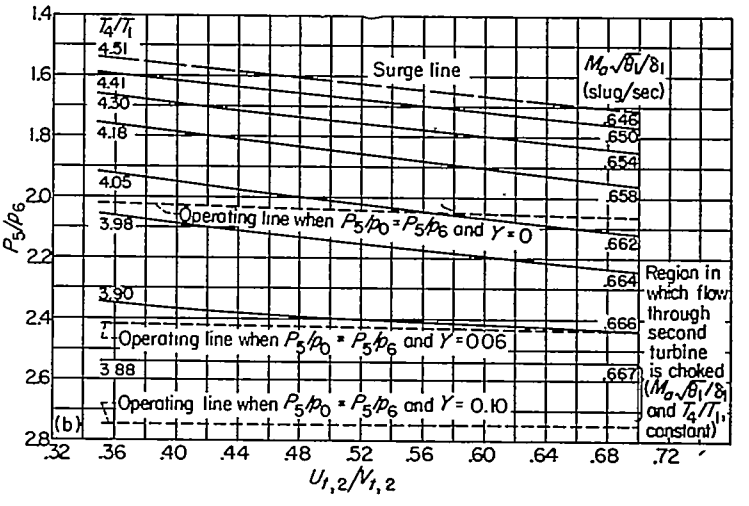

(b) $U_d/\sqrt{\theta_1}$, 1006 feet per second.

FIGURE 16.—Concluded. Relation between operating parameters of second turbine and gas generator.

The over-all performance values of the engine which have been superimposed on figure 16 are shown in figure 17. The values of the total-thrust-horsepower factor $thp/\sqrt{\theta_1}\delta_1$, the specific fuel consumption, the propeller efficiency η_p, and second-turbine efficiency $\eta_{t,2}$ at any values of $U_{t,2}/V_{t,2}$ and P_5/p_6 are shown in figure 17 (a) for $Y=0.10$ (Mach number, 0.71) and compressor tip-speed factor of 1062 feet per second. Figure 17 (b) is for $U_d/\sqrt{\theta_1}=1062$ feet per second and $Y=0.06$ (Mach number, 0.55); figure 17 (c), for $U_d/\sqrt{\theta_1}=1006$ feet per second and $Y=0.10$; and figure 17 (d), for $U_d/\sqrt{\theta_1}=1006$ feet per second and $Y=0.06$. The curves of $\eta_{t,2}$, which are functions of $U_{t,2}/V_{t,2}$ and P_5/p_6 only, are the same for all plots of figure 17 and hence are given only in figure 17 (a). In order to evaluate η_p, values of $D_p=13$ feet and $U_{t,2}/N_p=80$ (ft/sec)/rps were selected for the engine.

These figures show the effect of varying P_5/p_6 and $U_{t,2}/V_{t,2}$ on the over-all performance of the engine. In the range of values of $U_{t,2}/V_{t,2}$ from 0.45 to 0.60 and over the entire range of values of P_5/p_6 shown in figure 17, the maximum variation in $thp/\sqrt{\theta_1}\delta_1$ is about 15 percent and the maximum variation in specific fuel consumption about 20 percent. In this range of values of $U_{t,2}/V_{t,2}$ (0.45 to 0.60) and P_5/p_6, the values of turbine efficiency and propeller efficiency do not vary appreciably. At low values of P_5/p_6, the power output is large, mainly because the operating T_4/T_1 is high. However, the percentage of propeller-shaft power to total power available as useful work is much less than the optimum value. Increasing P_5/p_6 improves the efficiency of the power distribution between the propeller and the jet, which together with an accompanying improvement in compressor efficiency leads to decreased specific fuel consumption of the engine.

The effect of flight speed on performance factors is slight at both tip-speed factors shown. The total-thrust-horsepower factor increases slightly, and the specific fuel consumption decreases slightly with increased flight speed. It should be noted that, inasmuch as the factors θ_1 and δ_1 both increase with flight speed, the values of thrust horsepower increase much more than the values of $thp/\sqrt{\theta_1}\delta_1$. At a given

$M_a\sqrt{\theta_1}/\delta_1$ or T_4/T_1, the specific fuel consumption decreases as flight speed increases mainly because of operation at higher values of T_4. At the lower flight speed, the propeller efficiency is less sensitive to a change in operating conditions and remains at a higher value over a large part of the operating range shown in figure 17.

The thrust-horsepower factor drops off rapidly as compressor tip-speed factor is reduced from 1062 to 1006 feet per second. This decrease is due to operation in a region of lower T_4/T_1, lower mass-flow factors, and lower compressor pressure ratios. The specific fuel consumption also suffers when the tip-speed factor is reduced, mainly because of the accompanying decreases in compressor pressure ratio and T_4/T_1. At a tip-speed factor of 1062 feet per second and $Y=0.10$, an optimum specific fuel consumption of about 0.60 pound per thrust-horsepower-hour is obtained, and the corresponding thrust-horsepower factor is about 2700 horsepower. At $U_c/\sqrt{\theta_1}$ of 1006 feet per second and $Y=0.10$, the optimum specific fuel consumption is about 0.64 pound per thrust-horsepower-hour, and the corresponding thrust-horsepower factor about 2200 horsepower.

The rapid drop in thrust-horsepower factor with compressor tip-speed factor is even more pronounced at the lower tip-speed factors, because the propeller is unsuited to handle efficiently the low shaft powers that accompany the lower tip-speed factors (this characteristic is not evident from engine-performance figures which are presented only for values of $U_c/\sqrt{\theta_1}$ of 1062 and 1006 ft/sec). This observation emphasized the fact that this type of engine is very largely a maximum compressor tip-speed engine. The use of a free-wheeling turbine to drive the propeller permits a wider range of propeller operating parameters for given engine operating conditions than does the single-turbine engine, because the speed of the second turbine is independent of compressor speed. Better propeller performance can thereby be obtained.

In order to obtain the operating ranges shown in the plots of figures 13 and 17, a variable-area exhaust nozzle is required. The effective exhaust-nozzle area corresponding to design conditions ($U_c/\sqrt{\theta_1}=1062$ ft/sec, $T_4/T_1=4.23$, $P_2/P_1=5.1$, $U_{t,2}/V_{t,2}=0.50$, and $P_5/p_6=2.6$ at $Y=0.10$) is 1.08 square feet (evaluated by the method described in appendix D). This constant-area line of operation is included on figure 17. At any given flight Mach number, each point on the gas-generator plot has a small range of exhaust-nozzle areas associated with it. Conversely, at any flight Mach number each exhaust-nozzle area corresponds to a small range of operation along any $U_c/\sqrt{\theta_1}$ line on figure 13. The entire region of operation for constant exhaust-nozzle area $A_n=1.08$ square feet over a range of compressor tip-speed factors is included between the dashed curves in figure 13 (a) for $Y=0.10$. Figure 17 shows that the design nozzle area

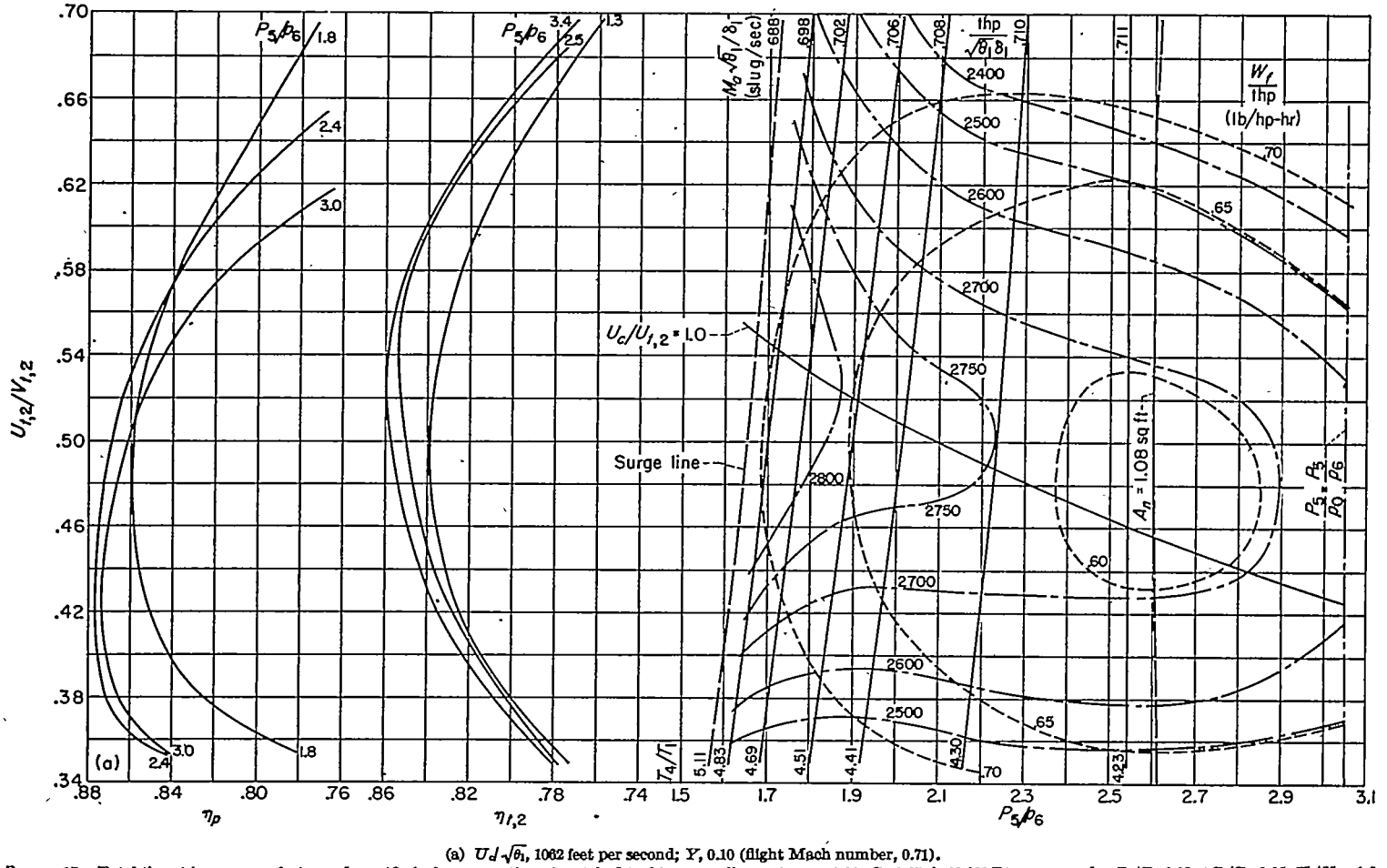

(a) $U_d\sqrt{\theta_1}$, 1062 feet per second; Y, 0.10 (flight Mach number, 0.71).

FIGURE 17.—Total-thrust-horsepower factor and specific fuel consumption of matched turbine-propeller engine; η_b, 0.96; C_s, 0.97; h, 18,900 Btu per pound; $\Delta P_d/P_1$, 0.03; $\Delta P_2/P_2$, 0.05; $U_d/U_{t,1}$, 1.0.

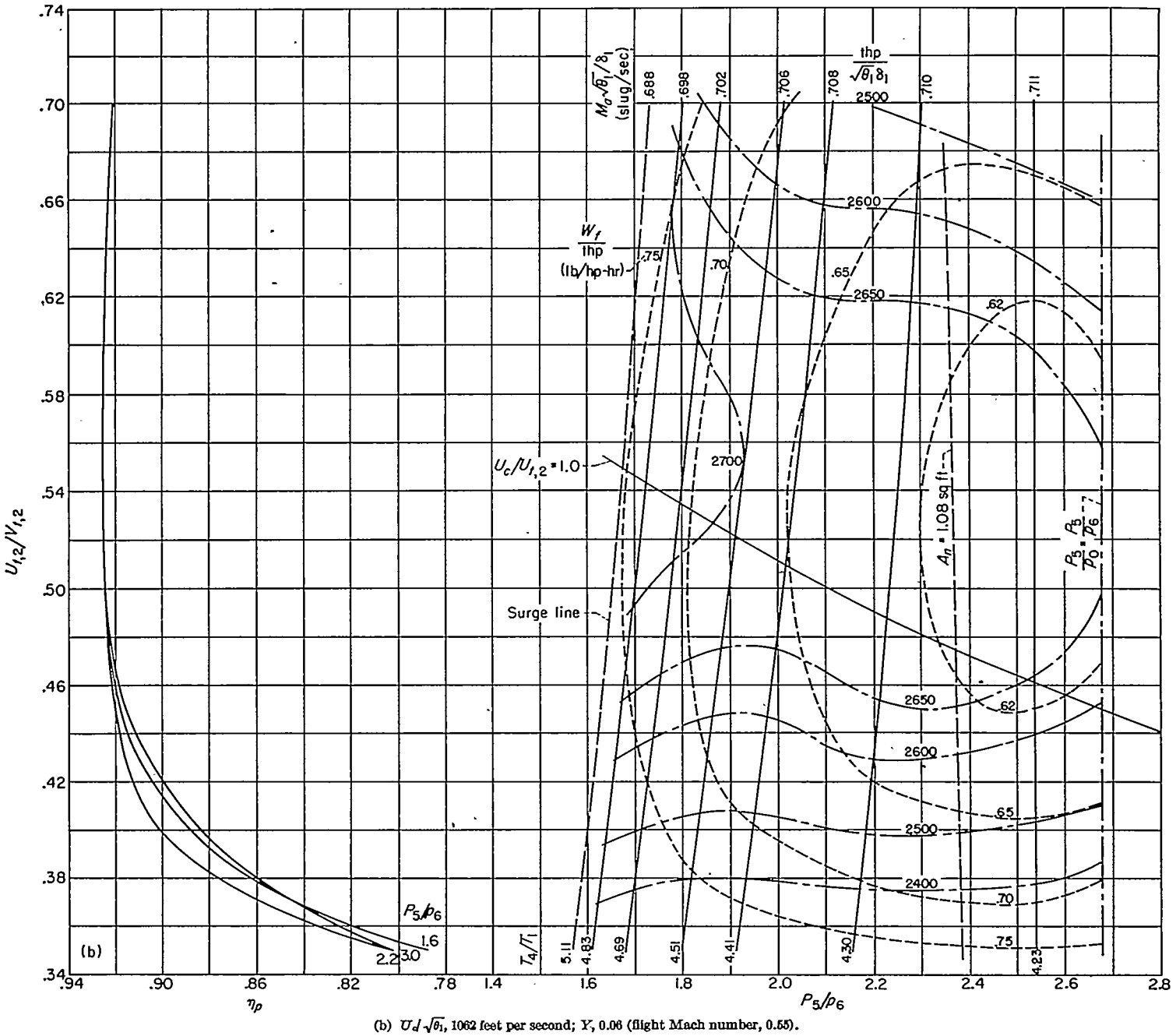

(b) $U_d/\sqrt{\theta_1}$, 1062 feet per second; Y, 0.06 (flight Mach number, 0.55).

FIGURE 17.—Continued. Total-thrust-horsepower factor and specific fuel consumption of matched turbine-propeller engine; η_s, 0.96; C_s, 0.97; h, 18,900 Btu per pound; $\Delta P_d/P_1$, 0.03; $\Delta P_3/P_3$, 0.05; $U_d/U_{t,1}$, 1.0.

of 1.08 square feet allows operation at almost optimum engine efficiency for the ranges of compressor tip-speed factor from 1006 to 1062 feet per second and of Y from 0.06 to 0.10 but at powers lower than maximum. The variable-area nozzle allows a much wider choice of combinations of economy and power than the fixed-area nozzle.

Temperature-stress limitations.—An important consideration in the determination of engine operating limits is the limitation due to excessive stresses in the turbine blades, which is a function of turbine pitch-line velocity, turbine-inlet temperature, and turbine design. The stresses in turbine blades are discussed in reference 7 for a range of pitch-line velocities for various turbine-blade designs and turbine sizes. Reference 8 shows the allowable stress of several turbine-blade materials as a function of temperature. In plots similar to figures 13 and 17, these factors must be taken into account in determining the regions of operation. Inasmuch as the value of the temperature at the turbine inlets for given temperature ratios T_4/T_1 and T_5/T_1 will vary with T_1, the limits of the operating regions imposed by strength considerations on these plots are functions of T_1.

The second turbine in the case of the divided turbine system can operate over a range of pitch-line velocities (or $U_{t,2}/V_{t,2}$) at any inlet temperature T_5. Therefore, at any T_4/T_1 or T_5/T_1 there may be some maximum value of $U_{t,2}/V_{t,2}$ that cannot be exceeded because of stress limitations; this maximum value increases as T_5 decreases. At lower values of compressor tip-speed factor, the problem of

limitation due to excessive stresses diminishes, particularly for the first turbine, which has a pitch-line velocity directly proportional to $U_c/\sqrt{\theta_1}$.

Performance of engine with connected turbine system.—The engine with both turbines connected is restricted to a fixed relation between turbine pitch-line velocity $U_{t,2}$ and compressor tip speed U_c. However, the power out of the first stage (the first turbine in the engine with divided turbine system) is no longer limited to being equal to compressor power. Some characteristics associated with the removal of the limit on turbine power distribution will now be discussed.

At any operating point on the compressor map (such as fig. 13), the corresponding values of T_4/T_1, $M_g\sqrt{\theta_4}/\delta_4$, and $M_g\sqrt{\theta_5}/\delta_5$ depend on the power output of the first turbine. When this power output is prescribed as in the case of the engine with divided turbine system (where the power output is always equal to the compressor power), these factors are all determined at every point. At a given $M_g\sqrt{\theta_5}/\delta_5$, the power output of the second turbine (or second stage) is limited by the range of P_5/p_6 possible at this mass-flow factor (see fig. 14). When the engine with a divided turbine system is operating at a given compressor point, it is thus limited to a range of power output of the second turbine, which depends on the corresponding value of $M_g\sqrt{\theta_5}/\delta_5$. The adjustment of the distribution of the available power

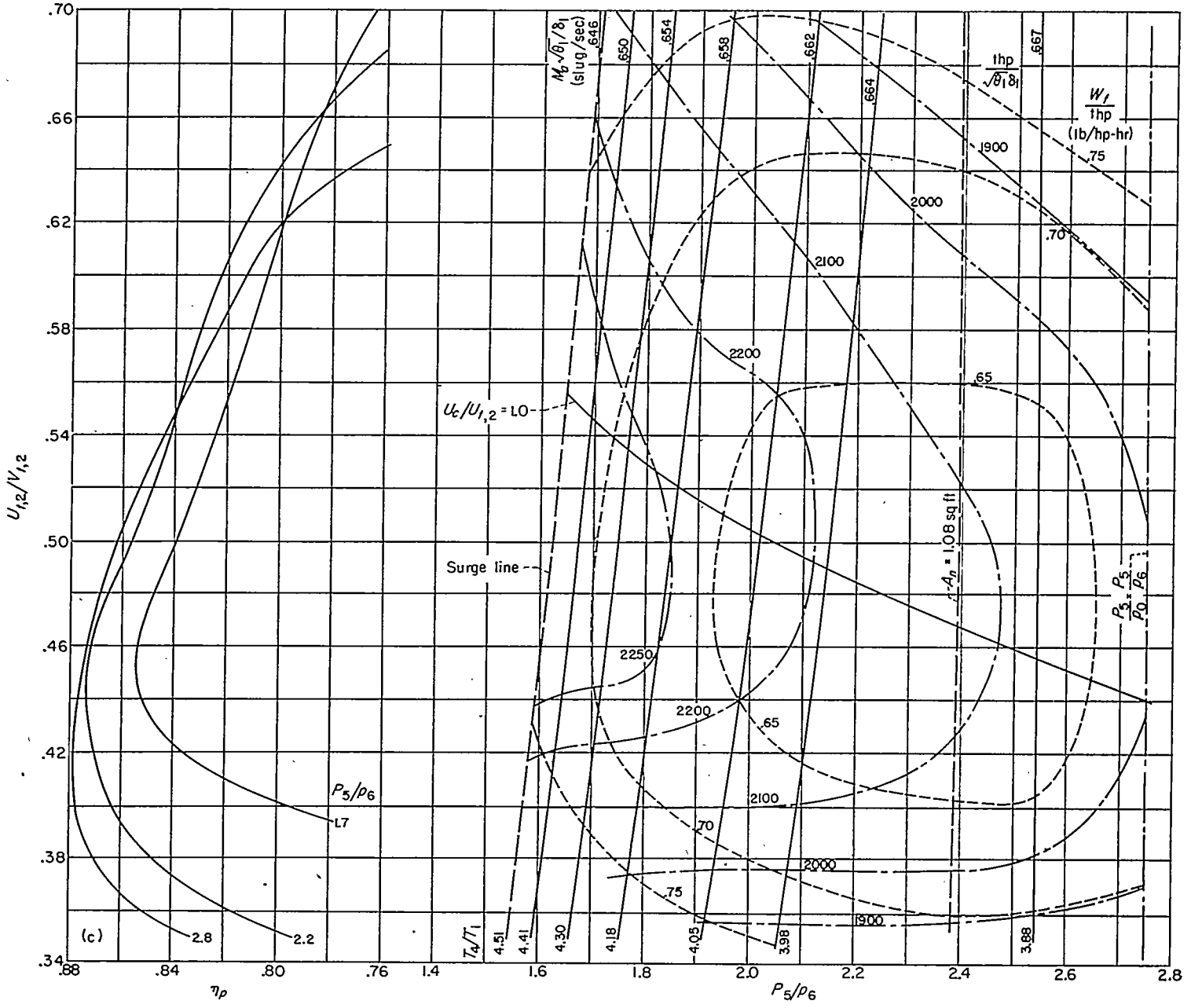

(c) $U_d/\sqrt{\theta_1}$, 1006 feet per second; Y, 0.10 (flight Mach number, 0.71).

FIGURE 17.—Continued. Total-thrust-horsepower factor and specific fuel consumption of matched turbine-propeller engine; η_b, 0.96 C_s, 0.97; h, 18,900 Btu per pound; $\Delta P_4/P_1$, 0.03; $\Delta P_2/P_2$, 0.05; $U_d/U_{t,1}$, 1.0.

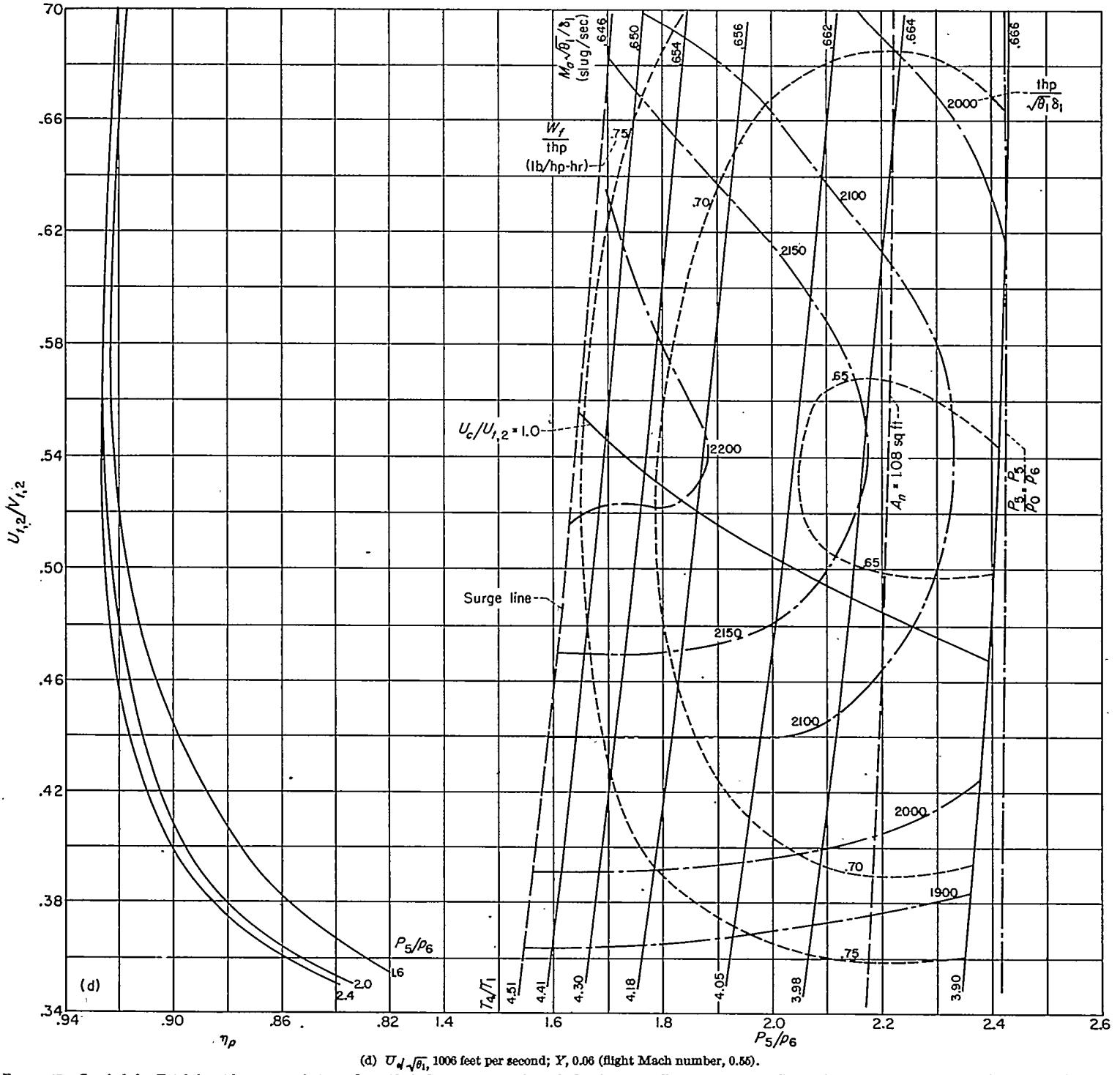

(d) $U_d/\sqrt{\theta_1}$, 1006 feet per second; Y, 0.06 (flight Mach number, 0.55).

FIGURE 17.—Concluded. Total-thrust-horsepower factor and specific fuel consumption of matched turbine-propeller engine; η_b, 0.96; C_s, 0.97; h, 18,900 Btu per pound; $\Delta P_d/P_1$, 0.03; $\Delta P_2/P_2$, 0.05; $U_d/U_{t,1}$ 1.0.

between the propeller and the exhaust-nozzle jet is thus often limited, and a low over-all engine efficiency may result at some off-design-point conditions. On the other hand, when the engine with connected turbines operates at a given compressor point, the values of T_4/T_1 and P_4/P_5 can be varied to give variable power output from the first turbine stage by an adjustment in fuel flow, exhaust-nozzle area, and propeller blade angle. This variation also leads to a range of values of $M_g\sqrt{\theta_5}/\delta_5$ that correspond to the given compressor operating point; hence, a larger range of power output may be obtained from the second-turbine stage. Power extraction from both turbines may then be adjusted to give more economical distribution of available power between propeller and exhaust jet than is possible with the divided turbine system, particularly at off-design operation.

Included in figure 17 are lines of operation for constant

$U_c/U_{t,2}=1.0$. This condition pertains to the operating line of an engine with the given connected turbine system having a fixed relation between $U_{t,2}$ and U_c and with the power output of the first-stage turbine equal to the compressor power. Figures 18 (a) and 18 (b) are performance plots of the engine similar to that of figure 17 (a), except that the power output of the first turbine is 3 and 7 percent greater, respectively, than the compressor power. These increases in power output of the first-stage turbine are obtained by increasing the combustion-chamber-outlet temperature T_4 and adjusting the exhaust-nozzle area and the propeller pitch; the range of values of the increase in turbine power is limited in order to avoid exceeding appreciably the design value of T_4. Operating conditions for these plots are the same as for figure 17 (a), namely $Y=0.10$ and $U_c/\sqrt{\theta_1}=1062$ feet per second. Lines of operation at

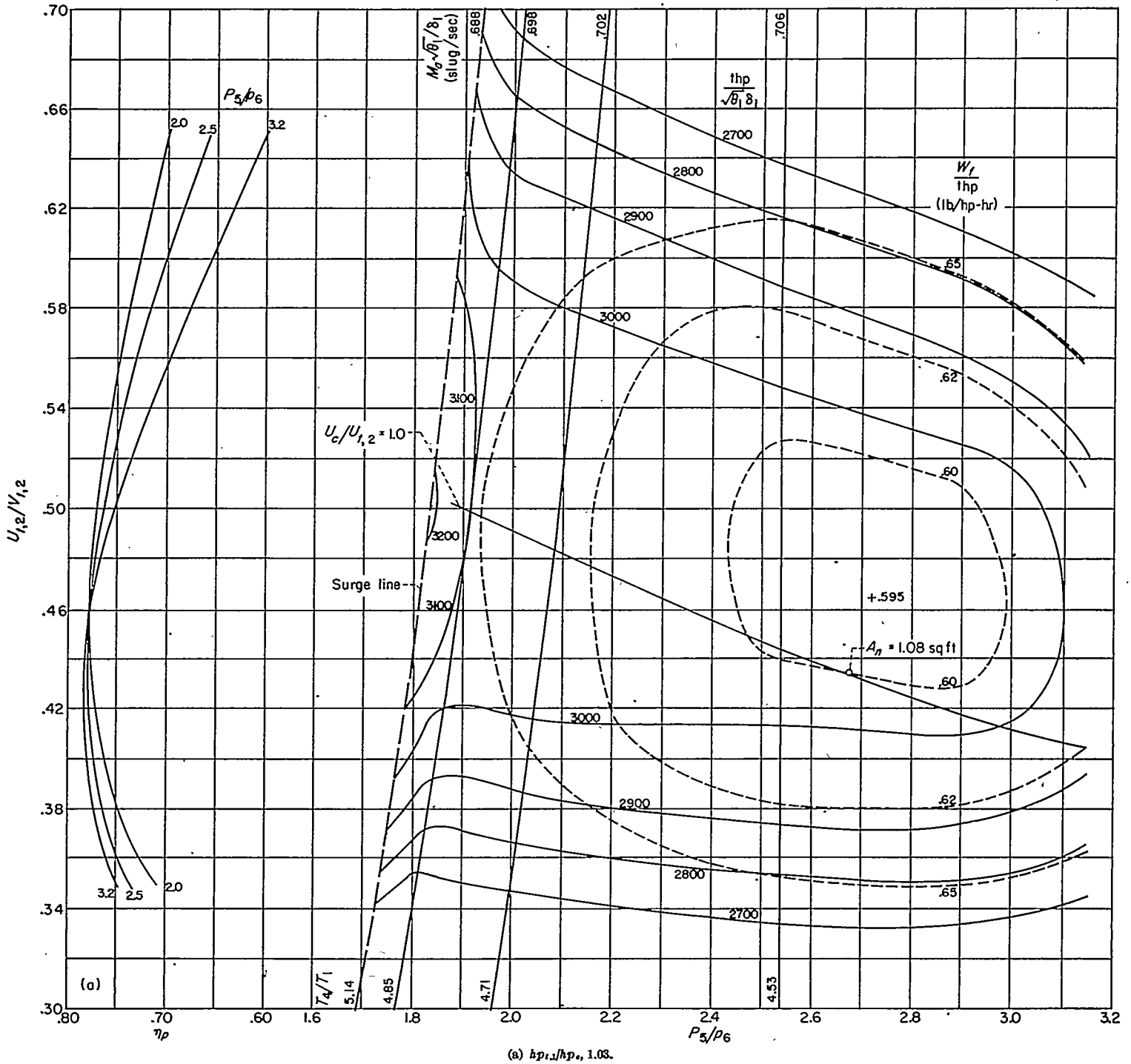

(a) $hp_{t,1}/hp_c$, 1.03.

FIGURE 18.—Performance plots of matched turbine-propeller engine for various values of power output of first turbine to compressor power; $U_d/\sqrt{\theta_1}$, 1062 feet per second; Y, 0.10 (flight Mach number, 0.71); η_b, 0.96; C_s, 0.97; h, 18,900 Btu per pound; $\Delta P_d/P_1$, 0.03; $\Delta P_3/P_2$, 0.05; $U_d/U_{t,1}$, 1.0.

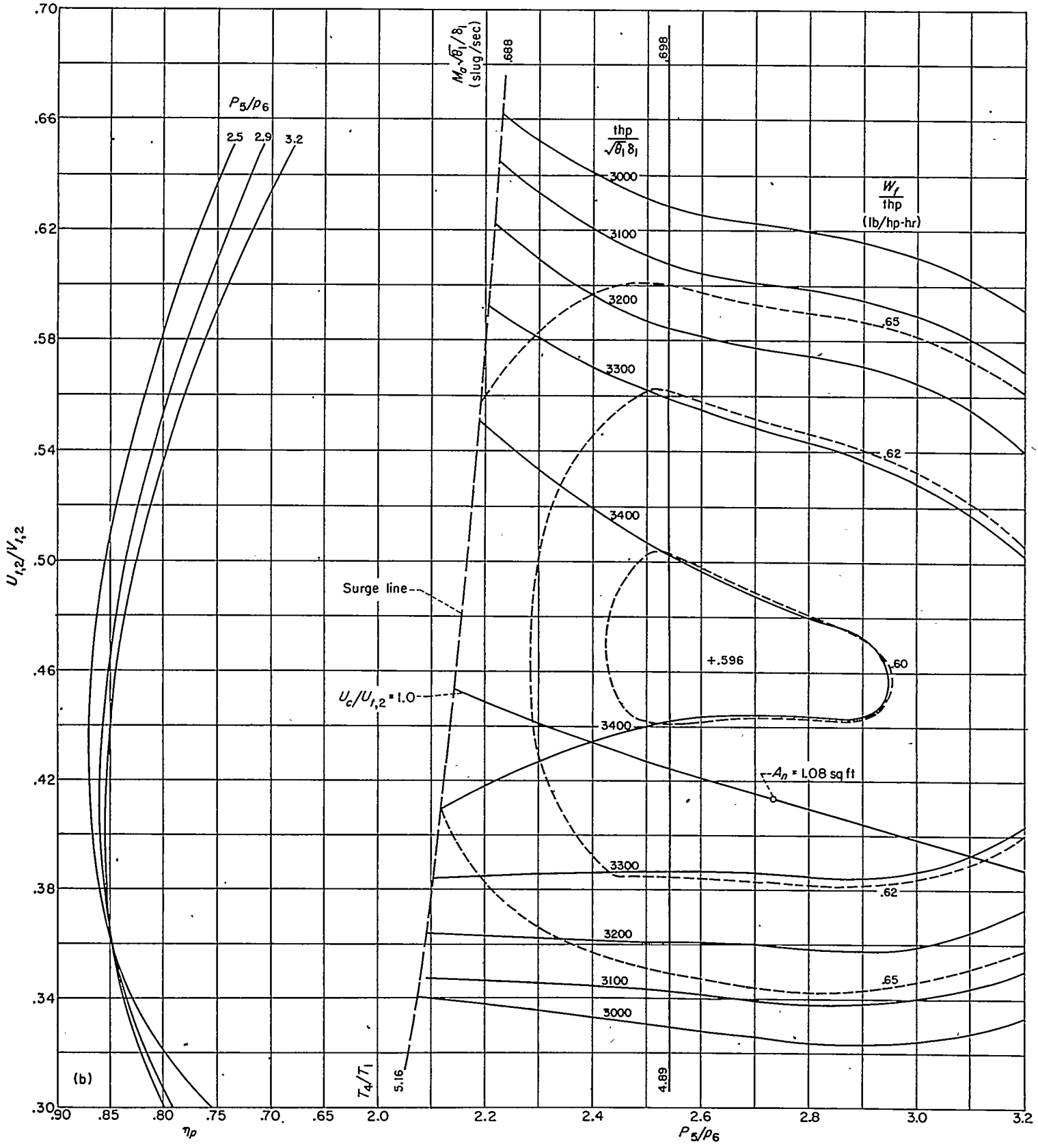

(b) $hp_{1,1}/hp_c$, 1.07.

FIGURE 18.—Continued. Performance plots of matched turbine-propeller engine for various values of power output of first turbine to compressor power; $U_d/\sqrt{\theta_1}$, 1062 feet per second; Y, 0.10 (flight Mach number, 0.71); η_b, 0.96; C_v, 0.97; h, 18,900 Btu per pound; $\Delta P_d/P_1$, 0.03; $\Delta P_2/P_2$, 0.05; $U_c/U_{1,1}$, 1.0.

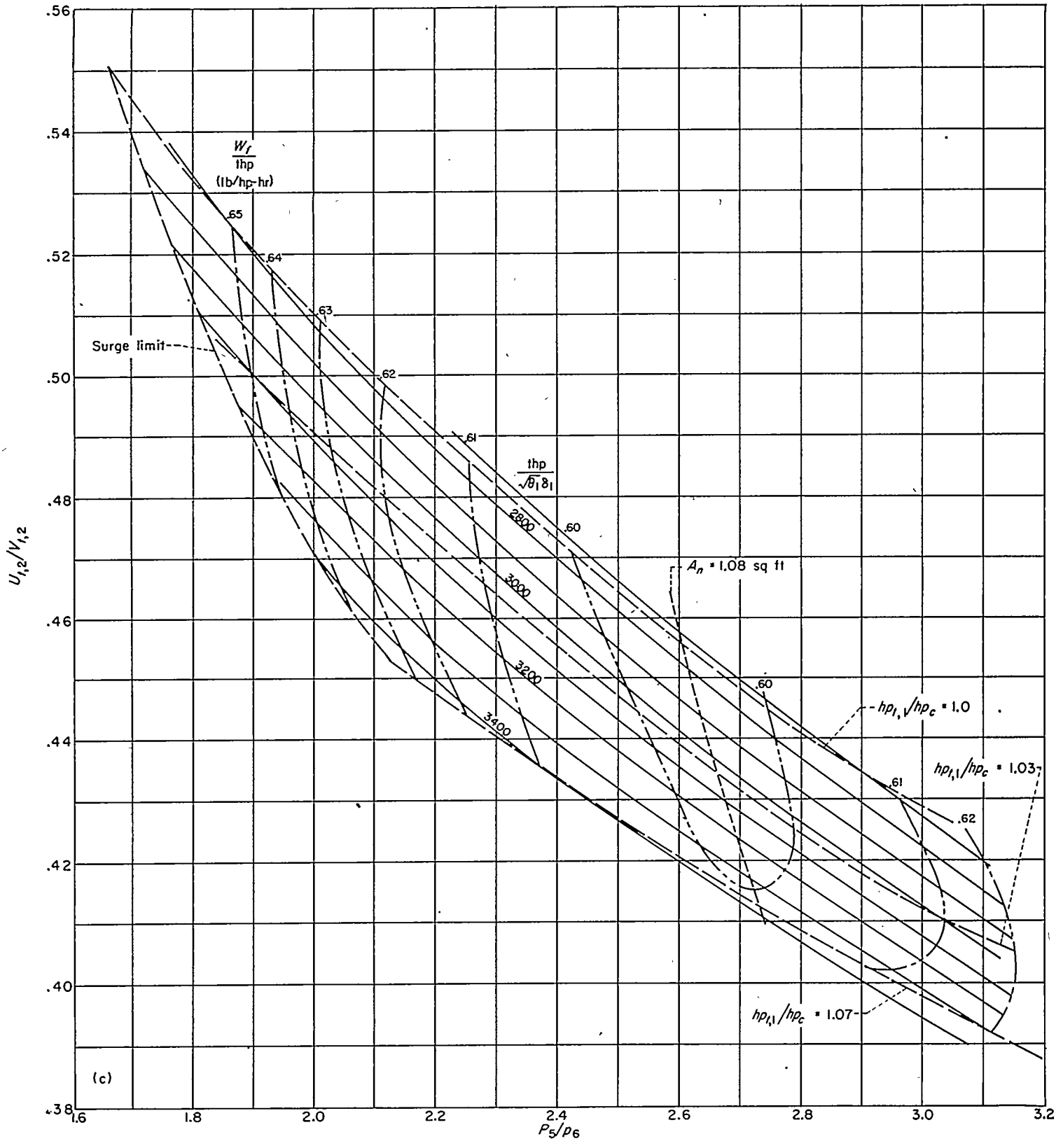

(c) $hp_{t,1}/hp_c$, 1.00 to 1.07; $U_d/U_{t,2}$=1.0.

FIGURE 18.—Concluded. Performance plots of matched turbine-propeller engine for various values of power output of first turbine to compressor power; $U_d/\sqrt{\theta_1}$, 1062 feet per second; Y, 0.10 (flight Mach number, 0.71); η_b, 0.96; C_s, 0.97; h, 18,900 Btu per pound; $\Delta P_d/P_1$, 0.03; $\Delta P_3/P_3$, 0.05; $U_d/U_{t,1}$, 1.0.

$U_c/U_{t,2}=1.0$ are again located on these plots and represent the case of the engine with connected turbines under consideration.

The operating lines for $U_c/U_{t,2}=1.0$ of figures 17 (a), 18 (a), and 18 (b) and the corresponding engine performance are shown on a single plot in figure 18 (c). This figure shows the effect on total power and specific fuel consumption due to varying the values of the ratio of the power output of the first turbine to the compressor power $hp_{t,1}/hp_c$ from 1.00 to 1.07. Operation over this range of values of $hp_{t,1}/hp_c$ is possible for the engine with connected turbines, whereas the divided turbine system limits engine operation to a value of $hp_{t,1}/hp_c=1.00$. Figures 17 (a) and 18 show that the engine with connected turbine system can achieve high power increases and maintain good economy by increasing the value of T_4/T_1. This desirable performance characteristic is possible because efficient distribution of power between propeller and jet is obtained at higher temperature ratios by extracting more power from the first turbine stage, which (by causing a higher value of $M_5\sqrt{\theta_5}/\delta_5$, which is accompanied by an increase in pressure differential across the second turbine) permits greater power output from the second turbine. For the engine with connected turbines illustrated, approximately a 20-percent increase in the total power output is obtained by increasing the T_4/T_1 from 4.23 (the design-point value) to 4.89 and increasing the value of $hp_{t,1}/hp_c$ from 1 to 1.07 with an increase in specific fuel consumption of only 1 percent. On the other hand, the engine with a divided turbine achieves an increase in total power of about 5 percent for this same change in T_4/T_1 (see fig. 17 (a)), while the specific fuel consumption increases about 17 percent.

For the conditions shown in figures 17 (a) and 18, the propeller and turbine efficiencies for the engine with the connected turbines are not appreciably decreased by restrictions imposed by the fixed relation among U_c, $U_{t,1}$, and $U_{t,2}$ for the interesting operating range. (The turbine efficiencies in fig. 17 (a) apply to fig. 18.)

Operation over the entire region shown in figure 18 (c) requires a variable-area exhaust nozzle. The line of constant A_n of 1.08 square feet is included in this figure. For the particular operating conditions covered in this figure, it is seen that this constant exhaust-nozzle area permits operation to be maintained at best efficiency for a range of powers including maximum power. With A_n of 1.08 square feet, the engine with a connected turbine can operate at $U_c/\sqrt{\theta_1}=$ 1062 feet per second from the surge line to the limiting line at which $M_5\sqrt{\theta_5}/\delta_5=0.60$ slug per second. At other values of compressor tip-speed factor, the region of operation on the compressor map with constant-area exhaust nozzle is much greater for the engine with a connected turbine than for the engine with a divided turbine.

SUMMARY OF RESULTS

For a series of turbine-propeller engines in which the appropriate components are used to give the design-point conditions and efficiencies, the following results were obtained:

1. At a given set of operating conditions, maximum thrust per unit mass rate of air flow and maximum thrust horsepower per unit mass rate of air flow occurred at a lower compressor pressure ratio than that at which minimum specific fuel consumption occurred.

2. An increase in combustion-chamber-outlet temperature caused an increase in power output per unit mass rate of air flow. Improved specific fuel consumption was obtained with increased combustion-chamber-outlet temperature, provided that the compressor pressure ratio was correspondingly increased.

3. An optimum jet velocity existed which gave best distribution between propeller-shaft power and jet power for maximum thrust horsepower and efficiency.

The following results were obtained from a study of two turbine-propeller engines, one engine having a divided turbine system in which the first turbine drove only the compressor and the second turbine independently drove the propeller, and the other engine having a connected turbine system which drove both the compressor and the propeller:

1. The connected turbine system offered greater adjustment of distribution of available power to the propeller shaft and the exhaust-nozzle jet, thereby permitting more efficient power distribution at off-design-point operation.

2. The divided turbine system offered more flexible control of component rotational speeds, which enabled speed adjustment giving best combination of turbine and propeller efficiencies.

3. When equipped with a constant-area exhaust nozzle, the engine with the divided turbine system was limited to a very narrow region of operation on the compressor operating diagram, whereas the engine with the connected turbine system was capable of a wide range of compressor operation.

LEWIS FLIGHT PROPULSION LABORATORY
NATIONAL ADVISORY COMMITTEE FOR AERONAUTICS
CLEVELAND, OHIO, *August 2, 1951*

APPENDIX A

DERIVATION OF PERFORMANCE EQUATIONS AND MISCELLANEOUS EXPRESSIONS

In addition to those symbols previously listed, the following symbols are used in these derivations:

$\bar{c}_p$ average specific heat at constant pressure of gases during combustion process, Btu/(slug)(°F) (This term, when used with the temperature change during combustion, is used to determine fuel consumption.)

H_0 enthalpy of air corresponding to ambient-air temperature t_0, Btu/slug

H_2 enthalpy of air corresponding to compressor-outlet total temperature T_2, Btu/slug

P_0 free-stream total pressure, lb/sq ft abs

R_a gas constant of air, 1716 ft-lb/(slug)(°F)

R_g gas constant of exhaust gas, ft-lb/(slug)(°F)

T_6 total temperature at outlet of second turbine, °R

X' factor equal to $\left[\frac{P_2/P_1}{(P_2/P_1)_{ref}}\right]^{\frac{\gamma_a-1}{\gamma_a}}$ or $(X)^{\frac{\gamma_a-1}{\gamma_a}}$

W_{th} ideal work for adiabatic process, ft-lb/slug

The jet velocity is given by

$$\frac{V_j^2}{C_v^2}=2Jc_{p,g}T_4\left[1-\left(\frac{p_0}{P_4}\right)^{\frac{\gamma_g-1}{\gamma_g}}\right]-\frac{550hp_t}{\frac{1}{2}M_a(1+f)\eta_t} \tag{A1}$$

$$\left(1-\frac{p_0}{P_4}\right)^{\frac{\gamma_g-1}{\gamma_g}}=1-\left(\frac{p_0}{P_2}\right)^{\frac{\gamma_g-1}{\gamma_g}}\left(1-\frac{\Delta P_2}{P_2}\right)^{-\frac{\gamma_g-1}{\gamma_g}} \tag{A2}$$

and when the last term is expanded into a series,

$$\left(1-\frac{\Delta P_2}{P_2}\right)^{-\frac{\gamma_g-1}{\gamma_g}}=1+\frac{\gamma_g-1}{\gamma_g}\frac{\Delta P_2}{P_2} \tag{A3}$$

for small $\frac{\Delta P_2}{P_2}$.

By the use of equations (A2) and (A3),

$$c_{p,g}\left[1-\left(\frac{p_0}{P_4}\right)^{\frac{\gamma_g-1}{\gamma_g}}\right]=c_{p,g}\left[1-\left(\frac{p_0}{P_2}\right)^{\frac{\gamma_g-1}{\gamma_g}}-\left(\frac{p_0}{P_2}\right)^{\frac{\gamma_g-1}{\gamma_g}}\left(\frac{\gamma_g-1}{\gamma_g}\right)\frac{\Delta P_2}{P_2}\right] \tag{A4}$$

Let

$$K=\frac{c_{p,g}\left[1-\left(\frac{p_0}{P_2}\right)^{\frac{\gamma_g-1}{\gamma_g}}\right]}{c_{p,a}\left[1-\left(\frac{p_0}{P_2}\right)^{\frac{\gamma_a-1}{\gamma_a}}\right]} \tag{A5}$$

and

$$K'=\frac{\left(\frac{p_0}{P_2}\right)^{\frac{\gamma_g-1}{\gamma_g}}\left(\frac{\gamma_g-1}{\gamma_g}\right)c_{p,g}}{\left(\frac{p_0}{P_2}\right)^{\frac{\gamma_a-1}{\gamma_a}}\left(\frac{\gamma_a-1}{\gamma_a}\right)c_{p,a}} \tag{A6}$$

When equations (A4) to (A6) are used in equation (A1),

$$\frac{V_j^2}{C_v^2}=2Jc_{p,a}T_4\left\{\left[1-\left(\frac{p_0}{P_2}\right)^{\frac{\gamma_a-1}{\gamma_a}}\right]K-\left(\frac{p_0}{P_2}\right)^{\frac{\gamma_a-1}{\gamma_a}}\left(\frac{\gamma_a-1}{\gamma_a}\right)\frac{\Delta P_2}{P_2}K'\right\}-\frac{550hp_t}{\frac{1}{2}M_a(1+f)\eta_t} \tag{A7}$$

Define

$$Y=\frac{V_0^2}{2Jc_{p,a}t_0} \tag{A8}$$

The total temperature at the compressor inlet (which is equal to the total temperature of the inlet air) is

$$T_1=t_0+\frac{V_0^2}{2Jc_{p,a}}=t_0(1+Y) \tag{A9}$$

The ratio of the ideal stagnation pressure P_0 to the ambient-air pressure is

$$\frac{P_0}{p_0}=\left(\frac{T_1}{t_0}\right)^{\frac{\gamma_a}{\gamma_a-1}}=(1+Y)^{\frac{\gamma_a}{\gamma_a-1}} \tag{A10}$$

The ratio of the actual total pressure at compressor inlet to the ambient-air pressure is

$$\frac{P_1}{p_0}=\frac{P_0-\Delta P_d}{p_0}=(1+Y)^{\frac{\gamma_a}{\gamma_a-1}}-\left(\frac{\Delta P_d}{P_1}\right)\left(\frac{P_1}{p_0}\right) \tag{A11}$$

from which

$$\frac{P_1}{p_0}=\frac{(1+Y)^{\frac{\gamma_a}{\gamma_a-1}}}{1+\frac{\Delta P_d}{P_1}} \tag{A12}$$

The compressor-shaft horsepower expressed as a function of compressor-inlet temperature and pressure ratio is

$$hp_c=\frac{M_a J c_{p,a} T_1}{550\eta_c}\left[\left(\frac{P_2}{P_1}\right)^{\frac{\gamma_a-1}{\gamma_a}}-1\right] \tag{A13}$$

where the specific heats of air during the compression process are assumed constant. Because of this assumption, the value of the compressor-shaft power calculated from equation (A13) for a given pressure ratio, inlet temperature, and efficiency is slightly greater than the actual compressor power. The deviation increases with increasing pressure ratio and inlet temperature. For values of T_1 up to 550° R and P_2/P_1 up to 40, the maximum error in compressor power is about 1 percent.

Define

$$Z=\frac{550hp_c}{M_a J c_{p,a} t_0} \tag{A14}$$

so that substituting equations (A9) and (A14) into equation (A13) results in

$$\frac{P_2}{P_1}=\left(1+\frac{\eta_c Z}{1+Y}\right)^{\frac{\gamma_a}{\gamma_a-1}}=\left(\frac{1+Y+\eta_c Z}{1+Y}\right)^{\frac{\gamma_a}{\gamma_a-1}} \tag{A15}$$

Equations (A12) and (A15) are combined so that

$$\left(\frac{p_0}{P_2}\right)^{\frac{\gamma_a-1}{\gamma_a}}=\frac{\left(1+\frac{\Delta P_d}{P_1}\right)^{\frac{\gamma_a-1}{\gamma_a}}}{1+Y+\eta_c Z} \tag{A16}$$

and expanding gives

$$\left(1+\frac{\Delta P_d}{P_1}\right)^{\frac{\gamma_a-1}{\gamma_a}}=1+\frac{\gamma_a-1}{\gamma_a}\frac{\Delta P_d}{P_1} \tag{A17}$$

which is accurate for small values of $\Delta P_d/P_1$.

From equations (A16) and (A17)

$$1-\left(\frac{p_0}{P_2}\right)^{\frac{\gamma_a-1}{\gamma_a}}=\frac{Y+\eta_c Z-\left(\frac{\gamma_a-1}{\gamma_a}\right)\frac{\Delta P_d}{P_1}}{1+Y+\eta_c Z} \tag{A18}$$

When equations (A16) to (A18) are substituted into equation (A7),

$$\frac{V_j^2}{C_*^2}=2Jc_{p,a}T_4\left[K\left(\frac{Y+\eta_c Z-\frac{\gamma_a-1}{\gamma_a}\frac{\Delta P_d}{P_1}}{1+Y+\eta_c Z}\right)-K'\left(\frac{\gamma_a-1}{\gamma_a}\right)\frac{\Delta P_2}{P_2}\left(\frac{1+\frac{\gamma_a-1}{\gamma_a}\frac{\Delta P_d}{P_1}}{1+Y+\eta_c Z}\right)\right]-\frac{550hp_t}{\frac{1}{2}M_a(1+f)\eta_t} \tag{A19}$$

The term involving the product of the pressure-drop ratios $\frac{\Delta P_d}{P_1}\frac{\Delta P_2}{P_2}$ can be neglected, so that equation (A19) becomes

$$\frac{V_j^2}{C_*^2}=\frac{2Jc_{p,a}T_4}{1+Y+\eta_c Z}\left[K\left(Y+\eta_c Z-\frac{\gamma_a-1}{\gamma_a}\frac{\Delta P_d}{P_1}\right)-K'\frac{\gamma_a-1}{\gamma_a}\frac{\Delta P_2}{P_2}\right]-\frac{550hp_t}{\frac{1}{2}M_a(1+f)\eta_t} \tag{A20}$$

The factor ϵ is defined by the equation

$$\frac{V_j^2}{C_*^2}=2Jc_{p,a}T_4\frac{Y+\eta_c Z}{1+Y+\eta_c Z}\epsilon-\frac{550hp_t}{\frac{1}{2}M_a(1+f)\eta_t} \tag{A21}$$

from which

$$\epsilon=K-K\left(\frac{\gamma_a-1}{\gamma_a}\right)\left(\frac{\Delta P_d}{P_1}\right)\left(\frac{1}{Y+\eta_c Z}\right)-K'\left(\frac{\gamma_a-1}{\gamma_a}\right)\left(\frac{\Delta P_2}{P_2}\right)\left(\frac{1}{Y+\eta_c Z}\right) \tag{A22}$$

Equation (A21) can be rewritten

$$\frac{hp_t}{M_a}=\left(\frac{T_4}{t_0}\epsilon\frac{Y+\eta_c Z}{1+Y+\eta_c Z}-\frac{V_j^2}{2C_*^2 Jc_{p,a}t_0}\right)\frac{\eta_t(1+f)Jc_{p,a}t_0}{550} \tag{A23}$$

The thrust horsepower developed by the propeller is

$$\frac{thp_p}{M_a}=\eta_p\left(\frac{hp_t}{M_a}-\frac{hp_c}{M_a}\right) \tag{A24}$$

and substituting equations (A14) and (A23) in (A24) yields

$$\frac{thp_p}{M_a}=\frac{\eta_p Jc_{p,a}t_0}{550}\left[\eta_t(1+f)\frac{T_4}{t_0}\epsilon\frac{Y+\eta_c Z}{1+Y+\eta_c Z}-\frac{V_j^2\eta_t(1+f)}{2C_*^2 Jc_{p,a}t_0}-Z\right] \tag{A25}$$

The thrust horsepower developed by the jet is

$$\frac{thp_j}{M_a}=[V_j(1+f)-V_0]\frac{V_0}{550} \tag{A26}$$

The total thrust horsepower of the engine is the sum of the propeller-thrust horsepower and jet-thrust horsepower; thus, from equations (A25) and (A26)

$$\frac{thp}{M_a}=\frac{\eta_p Jc_{p,a}t_0}{550}\left[\eta_t(1+f)\frac{T_4}{t_0}\epsilon\frac{Y+\eta_cZ}{1+Y+\eta_cZ}-\frac{V_j^2\eta_t(1+f)}{2C_v^2Jc_{p,a}t_0}-\frac{\eta_cZ}{\eta_c}\right]+[V_j(1+f)-V_0]\frac{V_0}{550} \tag{A27}$$

OPTIMUM JET VELOCITY AND η_cZ FOR MAXIMUM thp/M_a

For given values of V_0, η_p, η_t, η_c, T_4, t_0, and ϵ and with the component efficiencies and ϵ assumed to remain constant as η_cZ and V_j vary, optimum values of η_cZ and V_j are obtained from

$$\frac{\partial(thp/M_a)}{\partial(\eta_cZ)}=\frac{Jc_{p,a}t_0\eta_p}{550}\left[\eta_t(1+f)\frac{T_4}{t_0}\epsilon\frac{(1+Y+\eta_cZ)-(Y+\eta_cZ)}{(1+Y+\eta_cZ)^2}-\frac{1}{\eta_c}\right]=0 \tag{A28}$$

and

$$\frac{\partial(thp/M_a)}{\partial(V_j)}=\frac{Jc_{p,a}t_0\eta_p}{550}\left[-\frac{2V_j\eta_t(1+f)}{2C_v^2Jc_{p,a}t_0}\right]+\frac{V_0}{550}(1+f)=0. \tag{A29}$$

From equation (A29)

$$V_{j,opt}=V_0\frac{C_v^2}{\eta_t\eta_p} \tag{A30}$$

and from equation (A28)

$$1+Y+(\eta_cZ)_{ref}=\sqrt{\eta_c\eta_t(1+f)\epsilon\frac{T_4}{t_0}} \tag{A31}$$

where the term $(\eta_cZ)_{ref}$ is used to designate the value of η_cZ for which the thp/M_a given by equation (A27) is a maximum. Define

$$X'=\frac{1+Y+\eta_cZ}{\sqrt{\eta_c\eta_t(1+f)\epsilon\frac{T_4}{t_0}}} \tag{A32}$$

and

$$Y_j=\frac{V_j^2}{2Jc_{p,a}t_0} \tag{A33}$$

When equations (A32) and (A33) are substituted into equation (A25),

$$\frac{thp_p}{M_a}\frac{\eta_c}{\eta_p}\frac{519}{t_0}=\frac{519Jc_{p,a}}{550}\left[\eta_c\eta_t(1+f)\epsilon\frac{T_4}{t_0}-\left(X'+\frac{1}{X'}\right)\sqrt{\eta_c\eta_t(1+f)\epsilon\frac{T_4}{t_0}}+1+Y-Y_j\frac{\eta_t(1+f)\eta_c}{C_v^2}\right] \tag{A34}$$

The thrust produced by the propeller is

$$\frac{F_p}{M_a}=\frac{550}{V_0}\frac{thp_p}{M_a} \tag{A35}$$

Define the factor α as the ratio of the pounds of thrust produced by the propeller to the excess of turbine horsepower output over compressor horsepower input; then,

$$\alpha=\frac{F_p}{hp_t-hp_c} \tag{A36}$$

When equations (A35), (A36), and (A24) are combined,

$$\frac{F_p}{M_a}\left(\frac{519}{t_0}\right)\left(\frac{\eta_c}{\alpha}\right)=\frac{thp_p}{M_a}\left(\frac{519}{t_0}\right)\left(\frac{\eta_c}{\eta_p}\right) \tag{A37}$$

This equation permits the propeller thrust to be evaluated from equation (A34) when $V_0=0$ (at which velocity $\eta_p=0$ and $thp_p=0$).

For the case of $V_0=0$, the expression for optimum jet velocity (for optimum thrust) similarly reduces to

$$V_{j,opt}=\frac{C_v^2}{\eta_t}\frac{550}{\alpha} \tag{A38}$$

when equations (A35), (A36), (A24), and (A30) are combined.

EVALUATION OF CORRECTION FACTOR ϵ

The factors a and b are defined as

$$a=\frac{\Delta P_d}{P_1}\frac{\gamma_a-1}{\gamma_a}\frac{1}{Y+\eta_cZ} \tag{A93}$$

and

$$b=\frac{\Delta P_2}{P_2}\frac{\gamma_a-1}{\gamma_a}\frac{1}{Y+\eta_c Z} \tag{A40}$$

When equations (A39) and (A40) are substituted into equation (A22),

$$\epsilon=K-Ka-K'b \tag{A41}$$

The terms K and K' are close to unity in value, whereas the values of a and b are small in comparison with unity; therefore only a small error is introduced by letting

$$\epsilon=K-a-b \tag{A42}$$

The quantity c is defined as

$$c=K-1 \tag{A43}$$

then

$$\epsilon=1-a-b+c \tag{A44}$$

From equation (A5) and reference 9,

$$c=\frac{\frac{W_{th}}{T_4}}{Jc_{p,a}\left[1-\left(\frac{p_0}{P_2}\right)^{\frac{\gamma_a-1}{\gamma_a}}\right]}-1 \tag{A45}$$

where the values of W_{th}/T_4 are obtained from references 4 and 9 and unpublished data extending figure 9 of reference 9. These values correspond to the temperature T_4 and pressure ratio P_2/p_0.

FUEL CONSUMPTION

The expression for the fuel-air-ratio factor to obtain a rise in total temperature in the combustion chamber from T_2 to T_4 is

$$\eta_b f=\frac{\bar{c}_p(T_4-T_2)}{32.2h} \tag{A46}$$

where values of $\bar{c}_p$ are determined from reference 5.

From the conservation of energy,

$$H_2=H_0+\frac{V_0^2}{2J}+550\frac{hp_c}{M_a J} \tag{A47}$$

where H_2 is the enthalpy of the air corresponding to the compressor-outlet total temperature T_2 in Btu per slug. (Zero enthalpy is arbitrarily fixed at absolute zero temperature.) The symbol H_0 is the enthalpy of air corresponding to the ambient-air temperature t_0 in Btu per slug and is given by

$$H_0=c_{p,a}t_0 \tag{A48}$$

If equations (A48), (A8), and (A14) are used in equation (A47),

$$H_2=c_{p,a}t_0(1+Y+Z) \tag{A49}$$

Since T_2 is a function only of H_2,

$$T_2=\phi(H_2)=\phi[c_{p,a}t_0(1+Y+Z)] \tag{A50}$$

and the T_2 corresponding to the enthalpy H_2 is obtained from reference 4.

DERIVATION OF MISCELLANEOUS EXPRESSIONS

The pressure ratio $(P_2/P_1)_{ref}$ corresponding to any values of Y and $(\eta_c Z)_{ref}$ is, from equation (A15),

$$\left(\frac{P_2}{P_1}\right)_{ref}=\left[\frac{1+Y+(\eta_c Z)_{ref}}{1+Y}\right]^{\frac{\gamma_a}{\gamma_a-1}} \tag{A51}$$

or, substituting equation (A31) in equation (A51) gives

$$\left(\frac{P_2}{P_1}\right)_{ref}=\left[\eta_c\eta_t(1+f)\epsilon\frac{T_4}{t_0}\left(\frac{1}{1+Y}\right)^2\right]^{\frac{\gamma_a}{2(\gamma_a-1)}} \tag{A52}$$

From equations (A15), (A31), (A32), and (A51) it is seen that

$$X'=\left[\frac{P_2/P_1}{(P_2/P_1)_{ref}}\right]^{\frac{\gamma_a-1}{\gamma_a}} \tag{A53}$$

Define

$$X=\frac{P_2/P_1}{(P_2/P_1)_{ref}} \tag{A54}$$

then

$$X=(X')^{\frac{\gamma_a}{\gamma_a-1}} \tag{A55}$$

APPENDIX B

EQUATIONS FOR PERFORMANCE CHARTS

(The equation numbers correspond to those in the derivation given in appendix A.)

Figure 2 (a).—

$$Y=\frac{V_0^2}{2Jc_{p,a}t_0}=\frac{1}{2Jc_{p,a}519}\left(V_0\sqrt{\frac{519}{t_0}}\right)^2 \tag{A8}$$

$$\frac{P_0}{p_0}=\frac{P_1+\Delta P_d}{p_0}=(1+Y)^{\frac{\gamma_a}{\gamma_a-1}}=\left[1+\frac{1}{2Jc_{p,a}519}\left(V_0\sqrt{\frac{519}{t_0}}\right)^2\right]^{\frac{\gamma_a}{\gamma_a-1}} \tag{A10}$$

$$\text{Flight Mach number}=\frac{V_0}{\sqrt{\gamma_a R_a t_0}}=\frac{1}{\sqrt{\gamma_a R_a 519}}\left(V_0\sqrt{\frac{519}{t_0}}\right)$$

Figure 2 (b).—

$$Y_j=\frac{V_j^2}{2Jc_{p,a}t_0}=\frac{1}{2Jc_{p,a}519}\left(V_j\sqrt{\frac{519}{t_0}}\right)^2 \tag{A33}$$

Figure 3 (a).—

$$a=\frac{\Delta P_d}{P_1}\frac{\gamma_a-1}{\gamma_a}\frac{1}{Y+\eta_c Z} \tag{A39}$$

Figure 3 (b).—

$$b=\frac{\Delta P_2}{P_2}\frac{\gamma_a-1}{\gamma_a}\frac{1}{Y+\eta_c Z} \tag{A40}$$

Figure 3 (c).—

$$c=\frac{\frac{W_{th}}{T_4}}{Jc_{p,a}\left[1-\left(\frac{p_0}{P_2}\right)^{\frac{\gamma_a-1}{\gamma_a}}\right]}-1 \tag{A45}$$

where values of W_{th}/T_4 are obtained from references 4 and 9 and unpublished data extending data in reference 9.

Figure 4.—

$$\frac{P_2}{P_1}=\left(1+\frac{\eta_c Z}{1+Y}\right)^{\frac{\gamma_a}{\gamma_a-1}} \tag{A51}$$

$$\left(\frac{P_2}{P_1}\right)_{ref}=\left[\eta_c\eta_t\epsilon\frac{T_4}{t_0}\left(\frac{1}{1+Y}\right)^2\right]^{\frac{\gamma_a}{2(\gamma_a-1)}} \tag{A52}$$

In order to include the effect of added mass of fuel, the value of η_t used in equation (A52) should be the product $\eta_t(1+f)$.

Figure 5.—

$$\frac{thp_p}{M_a}\frac{\eta_c}{\eta_p}\frac{519}{t_0}=\frac{519\,Jc_{p,a}}{550}\left[\eta_c\eta_t\epsilon\frac{T_4}{t_0}-\left(X'+\frac{1}{X'}\right)\sqrt{\eta_c\eta_t\epsilon\frac{T_4}{t_0}}+1+Y-Y_j\frac{\eta_t\eta_c}{C_p^2}\right] \tag{A34}$$

where

$$X'=(X)^{\frac{\gamma_a-1}{\gamma_a}}$$

In order to include effect of added mass of fuel, the value of η_t used in equation (A34) should be the product $\eta_t(1+f)$.

Figure 6.—

$$H_2=c_{p,a}t_0(1+Y+Z) \tag{A49}$$

The T_2 corresponding to the enthalpy H_2 is obtained from reference 4.

Figure 7.—

$$\eta_b f=\frac{\bar{c}_p(T_4-T_2)}{32.2h} \tag{A46}$$

where $\bar{c}_p$ is determined from reference 5.

APPENDIX C

METHOD FOR DETERMINING OPERATING LINES OF CONSTANT T_4/T_1 AND CONSTANT $M_g\sqrt{\theta_5}/\delta_5$ FOR MATCHED SET OF TURBINE-PROPELLER-ENGINE COMPONENTS CONSISTING OF ONE TURBINE DRIVING ONLY COMPRESSOR AND SECOND TURBINE DRIVING ONLY PROPELLER

The procedure for plotting lines of constant T_4/T_1 and $M_g\sqrt{\theta_5}/\delta_5$ for the gas-generator plot of figure 13 (a) is as follows:

Equation (14), based on compressor power being equal to the power of first turbine, can be converted to

$$K_c\frac{U_c^2}{\theta_1}=\frac{1}{2}\frac{V_{t,1}^2}{\theta_4}\eta'_{t,1}\frac{T_4}{T_1} \tag{C1}$$

When T_4/T_1 is eliminated between equations (12) and (C1),

$$\sqrt{K_c}\frac{M_a\sqrt{\theta_1}}{\delta_1}\frac{U_c}{\sqrt{\theta_1}}=(1-r)\frac{P_2}{P_1}\frac{M_gV_{t,1}}{\delta_4}\sqrt{\frac{\eta'_{t,1}}{2}} \tag{C2}$$

(1) A point on figure 11 is selected at which the value of T_4/T_1 is desired. The values of $U_c/\sqrt{\theta_1}$, P_2/P_1, $M_a\sqrt{\theta_1}/\delta_1$, and K_c corresponding to the point are read on the figure.

(2) A value of $U_c/U_{t,1}$ is chosen based on sizes of turbine and compressor used; then, from the values of $U_c/U_{t,1}$ and K_c, $\sqrt{\eta'_{t,1}}/(U_{t,1}/V_{t,1})$ is evaluated from equation (15). A probable value of P_4/p_5 is assumed, and the value of $\sqrt{\eta'_{t,1}}/(U_{t,1}/V_{t,1})$ is used to read the values of $\eta_{t,1}$, $\eta'_{t,1}$, and $U_{t,1}/V_{t,1}$ from figure 12 (b).

(3) Equation (C2) is used to evaluate $M_gV_{t,1}/\delta_4$.

(4) Corresponding to the values of $M_gV_{t,1}/\delta_4$ and $U_{t,1}/V_{t,1}$, the values of $M_g\sqrt{\theta_4}/\delta_4$, $V_{t,1}/\sqrt{\theta_4}$, and P_4/p_5 are read on figure 12 (a). This value of P_4/p_5 should be used to check the values of η_t and $\eta'_{t,1}$ determined in step (2). If any appreciable differences in values of the efficiencies result, the revised value of $\eta'_{t,1}$ is used in step (3).

(5) The value of T_4/T_1 is now evaluated from equation (12).

In order to illustrate this method, the point is picked on figure 11 at which T_4/T_1 is to be evaluated.

(1) The point is selected where $U_c/\sqrt{\theta_1}=1006$ ft/sec, $P_2/P_1=4.74$, $M_a\sqrt{\theta_1}/\delta_1=0.660$ slug/sec, and $K_c=2.05$.

(2) A value of $U_c/U_{t,1}=1.0$ is used for this engine. When $U_c/U_{t,1}$ and K_c are used in equation (15), a value of $\sqrt{\eta'_{t,1}}/(U_{t,1}/V_{t,1})=2.02$ is obtained. This value is used in figure 12 (b), a value of P_4/P_5 of 2.0 is assumed; and the following values are read: $U_{t,1}/V_{t,1}=0.435$, $\eta_{t,1}=0.835$, and $\eta'_{t,1}=0.782$.

(3) From equation (C2) and an assumed value of $r=0.05$, a value of $M_gV_{t,1}/\delta_4=338$ ft/sec is calculated.

(4) When the values of $M_gV_{t,1}/\delta_4$ and $U_{t,1}/V_{t,1}$ are used in figure 12 (a), the following values are read: $V_{t,1}/\sqrt{\theta_4}=1136$ ft/sec, $M_g\sqrt{\theta_4}/\delta_4=0.298$ slug/sec, and $P_4/p_5=2.23$. This value of P_4/p_5 does not cause any appreciable change in values of turbine efficiencies from those determined in step (2) with an assumed value of P_4/p_5 of 2.0.

(5) The value of T_4/T_1 evaluated from equation (12) is 4.13.

In order to determine the total pressure at the turbine outlet, the following approximation of the turbine total efficiency is made:

$$\eta_{t,1}=\frac{550hp_{t,1}}{M_gJc_{p,g}T_4\left[1-\left(\frac{p_5}{P_4}\right)^{\frac{\gamma_g-1}{\gamma_g}}\right]-\frac{1}{2}M_gV_5^2}$$

$$=\frac{550hp_{t,1}}{M_gJc_{p,g}T_4\left[1-\left(\frac{p_5}{P_4}\right)^{\frac{\gamma_g-1}{\gamma_g}}\right]}$$

so that

$$\left.\begin{aligned}\eta_{t,1}Jc_{p,g}T_4\left[1-\left(\frac{p_5}{P_4}\right)^{\frac{\gamma_g-1}{\gamma_g}}\right]&=\eta'_{t,1}\frac{V_{t,1}^2}{2}\\ \text{or}\qquad 2Jc_{p,g}519\left[1-\left(\frac{p_5}{P_4}\right)^{\frac{\gamma_g-1}{\gamma_g}}\right]&=\frac{\eta'_{t,1}}{\eta_{t,1}}\frac{V_{t,1}^2}{\theta_4}\end{aligned}\right\} \tag{C3}$$

On figure 12 (a), the value of the upper abscissa $V_{t,1}/\sqrt{\theta_4}$ is related to the value of the lower abscissa P_4/p_5 according to the equation

$$2Jc_{p,g}519\left[1-\left(\frac{p_5}{P_4}\right)^{\frac{\gamma_g-1}{\gamma_g}}\right]=\frac{V_{t,1}^2}{\theta_4}$$

Figure 12 (a) can similarly be applied to equation (C3) by using the value of $\sqrt{\eta'_{t,1}/\eta_{t,1}}\ V_{t,1}/\sqrt{\theta_4}$ on the upper abscissa instead of $V_{t,1}/\sqrt{\theta_4}$ and reading the value of P_4/P_5 instead of P_4/p_5 on the lower abscissa.

The total-temperature ratio T_5/T_4 is

$$\frac{T_5}{T_4}=1-\frac{550\,hp_{t,1}}{Jc_{p,g}T_4M_g}=1-\frac{\eta'_{t,1}}{2}\frac{V^2_{t,1}}{\theta_4}\frac{1}{Jc_{p,g}519} \qquad \text{(C4)}$$

The mass-flow factor $M_g\sqrt{\theta_5}/\delta_5$ can now be obtained from equation (13).

In order to illustrate the calculations involved:

(6) From the values of $V_{t,1}/\sqrt{\theta_4}$, $\eta_{t,1}$, and $\eta'_{t,1}$ previously determined, $\frac{V_{t,1}}{\sqrt{\theta_4}}\sqrt{\frac{\eta'_{t,1}}{\eta_{t,1}}}=1100$ ft/sec. Corresponding to this value, $P_4/P_5=2.10$ is obtained.

(7) From equation (C4), a value of T_5/T_4 of 0.859 is obtained when a value of $c_{p,g}=8.9$ Btu/(slug)(°F) is assumed.

(8) Finally, from equation (13) a value of $M_g\sqrt{\theta_5}/\delta_5=0.581$ is determined.

APPENDIX D

METHOD FOR DETERMINING EXHAUST-NOZZLE AREA OF MATCHED SET OF TURBINE-PROPELLER-ENGINE COMPONENTS CONSISTING OF ONE TURBINE DRIVING ONLY COMPRESSOR AND SECOND TURBINE DRIVING ONLY PROPELLER

Useful equations for determining the values of several parameters needed in this method are as follows:

From the definition of effective exhaust-nozzle area,

$$M_g=A_n\left(\frac{p_0}{P_6}\right)^{\frac{1}{\gamma_g}}\rho_6\sqrt{2Jc_{p,g}T_6\left[1-\left(\frac{p_0}{P_6}\right)^{\frac{\gamma_g-1}{\gamma_g}}\right]}$$

where ρ_6 is the stagnation density at the second-turbine outlet and T_6, the total temperature at the outlet of the second turbine. Thus,

$$\frac{M_g\sqrt{\theta_6}}{A_n\delta_6}=\frac{2116}{\sqrt{519\,R_g}}\left(\frac{p_0}{P_6}\right)^{\frac{1}{\gamma_g}}\sqrt{2Jc_{p,g}\left[1-\left(\frac{p_0}{P_6}\right)^{\frac{\gamma_g-1}{\gamma_g}}\right]} \qquad \text{(D1a)}$$

Equation (D1a) is used until the critical pressure ratio is reached. The value of $M_g\sqrt{\theta_6}/A_n\delta_6$ remains constant thereafter, as p_0/P_6 becomes less than the critical pressure ratio. The mass-flow-per-unit-area factor for critical flow is

$$\frac{M_g\sqrt{\theta_6}}{A_n\delta_6}=\frac{2116}{\sqrt{519\,R_g}}\sqrt{\frac{2\gamma_g}{\gamma_g+1}\left(\frac{2}{\gamma_g+1}\right)^{\frac{2}{\gamma_g-1}}} \qquad \text{(D1b)}$$

Also, from energy considerations,

$$T_6=T_5-\frac{\eta'_{t,2}V^2_{t,2}}{2Jc_{p,g}}$$

from which

$$\frac{T_6}{T_5}=1-\frac{\eta'_{t,2}}{2Jc_{p,g}519}\left(\frac{V_{t,2}}{\sqrt{\theta_5}}\right)^2 \qquad \text{(D2)}$$

The procedure for determining the exhaust-nozzle area is as follows:

(1) For a given operating point, all conditions in the engine up to and including those at the second turbine are obtained by the method described in appendix C.

(2) For a given $M_g\sqrt{\theta_5}/\delta_5$, there can be a range of $U_{t,2}/V_{t,2}$ over which the second turbine can operate. At any $U_{t,2}/V_{t,2}$, the value of P_5/p_6 can be obtained from figure 14 (a), and $\eta'_{t,2}$ and $\eta_{t,2}$, from figure 14 (b).

(3) The total-pressure ratio P_5/P_6 is found by a method similar to that described in appendix C. From the value of P_5/p_6, the corresponding $V_{t,2}/\sqrt{\theta_5}$ is obtained on figure 14 (a); $\frac{V_{t,2}}{\sqrt{\theta_5}}\sqrt{\frac{\eta'_{t,2}}{\eta_{t,2}}}$ is then calculated and used to evaluate P_5/P_6.

(4) The pressure ratio $\frac{P_6}{p_0}=\left(\frac{P_6}{P_5}\right)\left(\frac{P_5}{P_4}\right)\left(\frac{P_4}{P_1}\right)\left(\frac{P_1}{p_0}\right)$ is evaluated, where P_1/p_0 is a function of flight Mach number and pressure loss in inlet duct (see equation (A12)).

(5) With suitable values for γ_g and $c_{p,g}$, the value of P_6/p_0 is used to calculate $M_g\sqrt{\theta_6}/A_n\delta_6$ from equation (D1a); equation (D1b) is used to calculate $M_g\sqrt{\theta_6}/A_n\delta_6$ if flow through the exhaust nozzle is choked.

(6) The values of $\eta'_{t,2}$ and $V_{t,2}/\sqrt{\theta_5}$ and an appropriate value of $c_{p,g}$ are used in equation (D2) to evaluate T_5/T_6.

(7) The value of A_n is then calculated from the identity

$$A_n=\frac{\frac{M_g\sqrt{\theta_5}}{\delta_5}\sqrt{\frac{T_6}{T_5}}\frac{P_5}{P_6}}{\frac{M_g\sqrt{\theta_6}}{A_n\delta_6}}$$

This method will be illustrated for the same operating point used in the illustration of appendix C:

(1) Some of the conditions corresponding to the given point of operation are $U_c/\sqrt{\theta_1}=1006$ ft/sec, $P_2/P_1=4.74$, $P_4/P_5=2.10$, and $M_g\sqrt{\theta_5}/\delta_5=0.581$ slug/sec.

(2) From the value of $M_g\sqrt{\theta_5}/\delta_5$ and a chosen value of 0.5 for $U_{t,2}/V_{t,2}$, the corresponding $P_5/p_6=1.91$ is obtained on figure 14 (a). Then from figure 14 (b) $\eta_{t,2}=0.850$ and $\eta'_{t,2}=0.796$.

(3) Corresponding to $P_5/p_6=1.91$, $V_{t,2}/\sqrt{\theta_5}=1032$ ft/sec is read on figure 14 (a). The parameter $\frac{V_{t,2}}{\sqrt{\theta_5}}\sqrt{\frac{\eta'_{t,2}}{\eta_{t,2}}}$ equal to 1000 ft/sec is evaluated, and the corresponding P_5/P_6 of 1.83 is read on figure 14 (a).

(4) The pressure ratio P_1/p_0 at a value of $Y=0.10$ and inlet pressure loss $\Delta P_d/P_1=0.03$ is 1.356 by equation (A12). Thus, $P_6/p_0=1.589$ is evaluated from the values of P_5/P_6, P_5/P_4, P_4/P_1, and P_1/p_0.

(5) From equation (D1a), values of $\gamma_g=1.35$ and R_g of 1720 ft-lb/(slug)(°F), and the value of P_6/p_0 previously determined, $M_g\sqrt{\theta_6}/A_n\delta_6=1.484$ (slug/sec)/sq ft is evaluated.

(6) The temperature ratio $T_6/T_5=0.877$ is obtained from $V_{t,2}/\sqrt{\theta_5}$, $\eta'_{t,2}$, and a value of $c_{p,g}=8.6$ Btu/(slug)(°F) in equation (D2).

(7) The value of the effective exhaust-nozzle area obtained by use of the identity given in step (7) is $A_n=0.67$ sq ft.

REFERENCES

1. English, Robert E., and Hauser, Cavour H.: A Method of Cycle Analysis for Aircraft Gas-Turbine Power Plants Driving Propellers. NACA TN 1497, 1948.
2. Mallinson, D. H., and Lewis, W. G. E.: The Part-load Performance of Various Gas-turbine Engine Schemes. War Emergency Issue No. 41 pub. by Inst. Mech. Eng. (London). (Reprinted in U. S. by A. S. M. E., April 1949, pp. 198–219.)
3. Pinkel, Benjamin, and Karp, Irving M.: A Thermodynamic Study of the Turbojet Engine. NACA Rep. 891, 1947. (Supersedes NACA WR E-241.)
4. Keenan, Joseph H., and Kaye, Joseph: Gas Tables. John Wiley & Sons, Inc., 1948.
5. Turner, L. Richard, and Bogart, Donald: Constant-Pressure Combustion Charts Including Effects of Diluent Addition. NACA Rep. 937, 1949. (Supersedes NACA TN's 1086 and 1655.)
6. Heidmann, Marcus F.: Method of Determining Conditions of Maximum Efficiency of an Independent Turbine-Propeller Combination. NACA TN 1951, 1949.
7. LaValle, Vincent L., and Huppert, Merle C.: Effects of Several Design Variables on Turbine-Wheel Weight. NACA TN 1814, 1949.
8. Grant, Nicholas J., Frederickson, A. F., and Taylor, M. E.: A Summary of Heat Resistant Alloys from 1200° to 1800° F. The Iron Age, vol. 161, no. 12, March 18, 1948, pp. 73–78; cont., vol. 161, no. 15, April 8, 1948, pp. 75–81; cont., vol. 161, no. 16, April 15, 1948, pp. 84–93.
9. Pinkel, Benjamin, and Turner, L. Richard: Thermodynamic Data for the Computation of the Performance of Exhaust-Gas Turbines. NACA WR–23, 1944. (Supersedes NACA ARR 4B25.)

(Unpublished Card) UNCLASSIFIED

ATI 139 567

(U. S. Military Organizations request copies from ASTIA-DSC. Others request copies from NACA, Wash., D.C.)

National Advisory Committee for Aeronautics, Lewis Flight Propulsion Lab., Cleveland, O. (NACA TN 2653)

A Thermodynamic Study of the Turbine-propeller Engine - and Appendixes A thru D - Technical Note

Pinkel, Benjamin; Karp, Irving M. 2 Aug'51 (March'52) 90pp diagr, graphs

Engines, Turboprop - Performance
Compressors - Matching
Engines - Thermodynamics

Power Plants, Jet and Turbine (5)
Performance (16)

27

UNCLASSIFIED